NASA Technical Memorandum 89131

Application of Formal Optimization Techniques in Thermal/Structural Design of a Heat-Pipe-Cooled Panel for a Hypersonic Vehicle

Charles J. Camarda
Langley Research Center
Hampton, Virginia

Michael F. Riley
PRC Kentron, Inc.
Hampton, Virginia

National Aeronautics
and Space Administration

Scientific and Technical Information Office

1987

Summary

Nonlinear mathematical programming methods are used to design a radiantly cooled and heat-pipe-cooled panel for a Mach 6.7 transport. The cooled portion of the panel is a hybrid heat-pipe/actively cooled design which uses heat pipes to transport the absorbed heat to the ends of the panel where it is removed by active cooling. The panels are optimized for minimum mass and to satisfy a set of heat-pipe, structural, geometric, and minimum-gage constraints. Two panel concepts are investigated: cylindrical heat pipes embedded in a honeycomb core and an integrated design which uses a web-core heat-pipe sandwich concept. The latter concept was lighter and resulted in a design which was less than 10-percent heavier than an all actively cooled concept. The heat-pipe concept, however, is redundant and can sustain a single-point failure, whereas the actively cooled concept cannot. An additional study was conducted to determine the optimum number of coolant manifolds per panel for a minimum-mass design.

Introduction

The use of nonlinear mathematical programming methods (formal optimization) for the synthesis of aeronautical and/or structural systems is fairly well established (refs. 1 and 2), but the use of such methods to design fluid-loop and/or heat-pipe systems has been limited (e.g., ref. 3). This paper is intended to demonstrate an efficient means for designing optimum, multifunction, heat-pipe systems using formal optimization methods, with the hope that such methods can replace cumbersome parametric methods (refs. 4 and 5).

The application chosen for study is the use of heat pipes to cool structural panels of a hypersonic cruise vehicle. This particular heat-pipe application was chosen for several reasons: it incorporates several disciplines of engineering analysis (thermodynamics, fluid dynamics, and structures), it is a viable application of heat pipes for future hypersonic vehicles, and it demonstrates a method for designing heat pipes to perform several functions efficiently (e.g., transport heat and support structural loads).

References 6 and 7 describe a combined radiantly and actively cooled panel (RACP) applicable to a Mach 6.7 hypersonic transport. The system uses heat shields and insulation to substantially reduce the incident heat load to the cooled structure and results in an overall structural design which is safer, more tolerant to off-design conditions, slightly lighter, and easier to fabricate than a design which must absorb all the incident heating. (See ref. 8.) However, the cooled structure remains susceptible to damage or leakage problems, which requires a redundant system, and hence additional weight and complexity, to avoid jeopardizing the flight of the vehicle. This paper is an investigation of the design of a heat-pipe-cooled panel which could replace the cooled-panel portion of the RACP described in references 6 and 7 (i.e., that portion of the panel between coolant inlet and outlet manifolds). An important advantage of using heat pipes for such an application is the increased redundancy in the design (e.g., if one heat pipe fails, the entire panel/vehicle will not be lost) with less weight penalty and system complexity. Heat pipes do not contain large quantities of working fluid, and if one should rupture, fluid leakage would cause minimal damage. Also, heat pipes naturally tend to eliminate any thermal gradients/stresses which might occur because of high localized heating.

Designs are obtained for several heat-pipe-cooled panels (HPCP) using formal optimization methods. In each design, heat pipes are used to transport the heat load experienced by the cooled panel to coolant manifolds located along the panel ends. The coolant manifolds for the heat-pipe-cooled panels contain both supply and return lines and circulate fluid and heat back to heat exchangers located on the vehicle. The effects of this redesigned manifold on total system mass and structural performance were not considered, and no attempt was made to include the coolant manifold design or coolant circulating system in the optimization. The panels are designed for minimum mass and to satisfy a set of heat-pipe, structural, geometric, and minimum-gage constraints. The first concept consists of cylindrical heat pipes embedded in a honeycomb sandwich structure. This design represents a retrofit, where the cylindrical heat pipes would replace the D-tubes of the previous RACP design. (See ref. 7.) It is not a truly integrated design (thermally and structurally), because the heat pipes, although capable of sustaining structural load, remain self-contained units which are bonded to the structure as opposed to being an integral part of the structure. Also, for this design the heat pipes are sized to satisfy heat-transport and fatigue requirements, and the sandwich panel is then resized to accommodate the structural loading. The fatigue requirement is satisfied by requiring the heat-pipe tube wall to be thicker than some minimum value. The second concept is a web-core heat-pipe sandwich panel which is optimized for minimum mass while subject to heat-pipe, strength, buckling, fatigue, and minimum-gage constraints. This concept represents an integrated heat-pipe/structural design where the heat pipe is an integral part of the structure and is designed for two

functions simultaneously—to transport heat and to support structural loads. Both panels were designed to withstand the same set of thermal/structural loading conditions and constraints as the RACP of reference 7. Further, the effect of additional, equally spaced coolant manifolds on optimized heat-pipe-panel mass was studied. The design methodology used in the present study to design the heat-pipe panel is compared with that presented in reference 7 for designing the RACP.

The optimizer used in the present study is CONMIN (ref. 9), which uses the method of feasible-directions algorithm for constrained function minimization. The optimizer is coupled to analysis and plotting modules via FRANNOP (a computer program described in ref. 10).

Symbols

A	cross-sectional area, in^2
a	crack length, in.
a_o	sonic velocity, in/sec
b	panel width, in.
D	groove depth, in.
D_x	panel bending stiffness, in-lb
da/dN	crack growth rate, in/cycle
E	modulus of elasticity, lb/in^2
F	objective function, lbm/in^2
FS	factor of safety
$f_{\max}, f_{\min}$	maximum and minimum cyclic stresses, ksi
g_c	gravitational constant, 386 lbm-in/lbf-sec^2
g_i	ith constraint
h	heat-transfer coefficient, Btu/ft^2-hr-°F
h_c	panel-core height, in.
I_x	moment of inertia about x-axis per unit width, in^3
K_c	stress-intensity factor, ksi-$\sqrt{in.}$
K_w	wick permeability, in^2
ΔK	stress-intensity range, ksi-$\sqrt{in.}$
L	panel length, in.
L_{eff}	effective length of heat pipe, in.
ℓ	simply supported plate length, in.
M	mass, lbm
$M_{x,\max}$	maximum panel bending moment per unit width, $\frac{\text{in-lbf}}{\text{in.}}$
m	number of half waves
N	number of load cycles
N_m	number of additional coolant manifolds
P	spacing between heat pipes or coolant tubes, in.
P_x	applied in-plane load in x-direction, lbf/in.
$P_{x,ob}$	overall panel buckling load per unit width, lbf/in.
p_v	internal pressure, lbf/in^2
Q	flaw shape parameter
Q_{AIN}, Q_{TIN}	axial and transverse heat input loads, Btu/sec
Q_{AW}, Q_{AS}, Q_{AE}	axial heat-pipe wicking, sonic, and entrainment limits, Btu/sec
Q_{IN}	input heat load to panel, Btu/sec
Q_{TW}	transverse heat-pipe wicking limit, Btu/sec
$Q_{x,\max}$	maximum panel shear load per unit width in x-direction, lbf/in.
q	uniform transverse panel load per unit area, lbf/in^2
$\dot{q}_{\text{abs}}$	absorbed heat input to cooled panel, Btu/ft^2-sec
R	stress ratio
r_1, r_2, r_3	heat-pipe radii shown in figure 6, in.
r_p	pore radius of wick, in.
r_v	hydraulic radius of heat pipe, in.
S	spacing of panel-core webs, in.
T	temperature, °F
t	plate thickness, in.

t_f, t_c	face-sheet and core thicknesses, in.
t_o	outer facing thickness, in.
t_s, t_w	screen and wick thicknesses, in.
V	static moment of area, in^3
W	groove width, in.
w	simply supported plate width, in.
X_i	ith design variable
y	distance from neutral axis, in.
β_2, β_5	coefficients
γ	ratio of specific heats
λ	latent heat of vaporization, Btu/lbm
μ	viscosity, lbm/sec-in.
υ	Poisson's ratio
ρ	mass density, lbm/in^3
σ_ℓ	liquid surface tension, lbf/in.
$\sigma_{x,\mathrm{FAT}}, \sigma_{x,p}, \sigma_{x,lb}, \sigma_{x,\max}, \sigma_{y,p}, \sigma_{tc}, \sigma_{x,f}, \tau_{zx,\max}$	stresses defined in structural analysis, lbf/in^2
$\sigma_{\mathrm{ult}}, \tau_{\mathrm{ult}}$	ultimate normal and shear stresses, lb/in^2
Φ_o	buckling parameter
Subscripts:	
c	core (web)
f	face sheet
ℓ	liquid
lb	local buckling of face sheet or webs
ob	overall panel buckling
ref	reference
s	solid
v	vapor
w	wick

Design Problem Description

A radiantly and actively cooled panel (RACP) was designed for a location 10 ft aft of the nose on the lower fuselage centerline of a Mach 6.7 hydrogen-fueled hypersonic transport described in reference 7. The design requirements and criteria for the RACP of reference 7 are discussed subsequently with a description of design methodologies for an RACP design and an alternative version of it, a radiantly and heat-pipe-cooled panel (RHPCP), which is a hybrid design using active cooling and heat pipes to cool the structural panel.

Design Loads and Criteria

Reference 7 describes the design requirements, design criteria, and design process for a full-scale 2- by 20-ft RACP, shown in figure 1. The high-heat-flux panel of reference 8 was designed for an incident heat flux of 12 Btu/ft^2-sec to a 300°F surface temperature. A heat-transfer coefficient of 16 Btu/ft^2-hr-°F and an adiabatic wall temperature of 3000°F were used in reference 7 to define the heating environment. These quantities were used to determine heat input to the surface of the RACP and heat absorbed $\dot{q}_{\mathrm{abs}}$ by the actively cooled-panel (ACP) portion of the RACP. It was determined in reference 7 that a minimum-mass design results for $\dot{q}_{\mathrm{abs}} = 0.8$ Btu/ft^2-sec. A uniform surface pressure of ± 1.0 psi and a cyclic, uniform, in-plane limit load of 1200 lbf/in. along the 2-ft edge comprised the structural loads on the panel. Design life for the RACP called for a 10 000-hr exposure to operational temperatures, 300°F for the aluminum ACP, and 20 000 cycles (5000 cycles with a scatter factor of four) of design limit loads. Stresses in the aluminum sandwich panel were restricted to values below which an initial flaw size of 0.005 in. at the edge of a fastener hole would not grow to a critical length and surface flaws of 0.005 in. would not grow through the thickness of the coolant tubes or manifolds during the 20 000 limit-load cycles. A factor of safety (FS) of 1.5 was applied to in-plane and transverse loads to obtain ultimate loads, and an FS of 4.0 was used to obtain ultimate burst-pressure loads. The radiantly and actively cooled panel was designed to sustain design limit loads without yielding and design ultimate loads without structural failure. For the heat-pipe-cooled-panel (HPCP) portion of the RHPCP, an FS of 1.5 was also applied to thermal loads to ensure thermal redundancy if a heat pipe failed.

Design Methodologies

Two different design methodologies were used to design a cooled panel: parametric and trade studies were used to design the RACP of reference 7, and nonlinear mathematical programming (formal optimization) techniques were used to design the hybrid actively cooled and heat-pipe-cooled panel of

the present study. Although the scope of the HPCP design study is limited, the study demonstrates the methodology as a viable alternative to parametric techniques, which are limited in effectively selecting an optimum design as the number of design variables increases.

The parametric and trade studies used to design the RACP of reference 7 are illustrated in figure 2. Figure 2(a) indicates the overall process, and figure 2(b) shows the numerous parametric and trade studies required to arrive at a final design. Because two mechanisms were used to accommodate the incident heating, i.e., rejection by radiation and absorption by convection, it was necessary to establish the performance of each subsystem (heat shield and actively cooled panel). By using simplified analyses and the series of trade studies shown in figure 2(b), it was determined that a minimum-mass system results when the cooled panel absorbs 0.8 Btu/ft^2-sec. Once the major parameters and absorbed heat flux were determined, more extensive analyses and trade studies were performed to substantiate the design, to size the cooling system, and to arrive at the minimum-mass cooled structural panel which could absorb 0.8 Btu/ft^2-sec.

The current investigation replaces part of the trade studies with nonlinear mathematical programming techniques to design a heat-pipe-cooled panel to replace the portion of the cooled panel between the coolant manifolds. Although this represents only a portion of the total RHPCP system, it is sufficient to demonstrate the methodology. For this problem, therefore, results of references 7 and 8 were used to determine the design and operating conditions. The absorbed heat load and maximum operating temperature were assumed to be 0.8 Btu/ft^2-sec and 300°F, respectively. The optimization procedure is illustrated in figure 3. The procedure is discussed in detail in the section entitled "Statement of the Optimization Problem."

Actively Cooled Panel (ACP) Description

The ACP, shown in figure 4, consists of an aluminum honeycomb-sandwich structural panel with coolant tubes (D-tubes) next to the outer skin. The honeycomb structural panel is cooled by a 60-percent mass solution of ethylene glycol in water pumped through the D-shaped cooling tubes at a flow rate of 3.4 gal/min. The panel is 2 by 20 ft and is supported by channel-section frames every 2 ft (representative of typical transport construction support) and has inlet and outlet coolant manifolds at the ends of the panel.

Heat-Pipe-Cooled Panel (HPCP) Description

The HPCP proposed in the present study differs from the ACP of reference 7 in two areas. Instead of an actively cooled structural panel (fig. 4), a passive, self-contained, heat-pipe-cooled panel (HPCP) is used to transport heat to coolant manifolds on either end of the panel. Also, the manifolds of the HPCP include both supply and return coolant lines and circulate fluid and heat back to heat exchangers located on the vehicle.

Heat pipes, shown schematically in figure 5, are self-contained devices which can transport heat nearly isothermally, at high rates, and over long distances (in this case 10 ft) without the need for external pumping. They operate by absorbing heat by the evaporation of a working fluid in a net heat input region, which in this case is the surface area of the panel. The heated vapor thus formed then flows to cooler condenser sections (actively cooled ends of the panel where coolant manifolds are located), where heat is rejected by the condensation of the vapor. The cycle is completed with the return flow of liquid condensate back to the heated region by the capillary action of the wick. Several fluid-dynamic limits which can prevent normal heat-pipe operation are described in appendix A.

The coolant manifolds on the HPCP would circulate the coolant along the ends of the panel, extracting heat from the heat pipes, and back to heat exchangers located in the vehicle interior instead of through the panel as is done on the ACP. It is assumed that there is no mass penalty associated with the redesigned coolant manifolds. The heat-pipe panel offers more redundancy than the ACP design, because adjacent heat pipes are sized to accommodate the additional heat load if a heat pipe fails. Hence, loss of one heat pipe would not cause leakage of large amounts of coolant, catastrophic overheating, and subsequent total panel failure and a mission abort or vehicle loss. Two heat-pipe-panel designs are investigated: one design simply replaces the D-tube coolant passages of reference 7 with cylindrical heat pipes (fig. 6), and the other is an integral heat-pipe/structural configuration called a web-core heat-pipe sandwich panel (fig. 7). Two variations of wick configurations were investigated for each design. Also, effects of adding more coolant manifolds, equally spaced along the panel, on the mass of the optimized panel were investigated.

Cylindrical heat pipes embedded in a honeycomb sandwich. Cylindrical heat pipes were chosen instead of D-shaped heat pipes because the net heat load to the panel is small enough that temperature gradients

between adjacent heat pipes are of little concern and because the line contact of the cylindrical tube is of no consequence. Also, for the heat-pipe design, the cross-sectional area must be sufficient to accommodate the axial heat transport, and the circular cross section offers more area than the D-shaped tubes. The honeycomb-sandwich dimensions were similar to those of the ACP, and the wall thickness of the heat pipes was maintained at 0.02 in. to satisfy fatigue constraints identified in reference 7. The heat pipes use a screen-covered, axial-grooved wick; the screen covering the grooves is a 165×1400 mesh screen with a pore radius r_p of 0.0009055 in. (ref. 11). An alternate wick which consisted of screen-covered corrugated channels where the channels and screen covering use the same 165×1400 mesh screen was also investigated. The latter configuration (referred to as corrugated sandwich screen wick) increases the cross-sectional liquid area but decreases the amount of load-carrying material. The material is aluminum, and the working fluid is toluene.

Heat-pipe web-core sandwich panel. The heat-pipe web-core sandwich panel design integrates the heat pipes with the structure to produce an efficient thermal/structural design. The web-core panel (fig. 7) consists of two face sheets of equal thickness t_f and channel-section webs of thickness t_c. Two wick concepts were investigated: screen-covered axial grooves (165×1400 mesh screen, fig. 7(a)) and closed channels formed by using a sandwich wick of corrugated screen bonded between a layer of flat screen (165×1400 mesh) and the inner surface of the face sheets (fig. 7(b)). Both concepts assume a composite screen wick along the webs to transport fluid to the heated face of the panel. The composite screen wick (fig. 7) is composed of one layer of high-density screen (165×1400 mesh) along the liquid/vapor interface against several layers of coarser screen (325×325 mesh) along the web walls. The material is aluminum, and the working fluid is toluene.

Statement of the Optimization Problem

The design of heat-pipe panels is posed as a nonlinear constrained mathematical optimization problem, where the objective function to be minimized is the panel mass per unit planform area. The constraints of the problem are the thermal, structural, geometric, and minimum gage requirements which the panel must satisfy. The design variables in each problem are selected cross-sectional dimensions of the panel.

The mathematical statement of the optimization problem is as follows: find the set of design variables X such that

$$F(X) \text{ minimum}$$
$$\text{subject to}$$
$$g_i(X) \leq 0$$

where F is the objective function, in this case panel mass per unit planform area; where the design variables X are various cross-sectional dimensions of the panel; and where the inequality constraints $g_i(X) \leq 0$ are various thermal/structural requirements or limits. The optimization algorithm used in the present study is CONMIN (ref. 9), which is a general-purpose optimization program that performs constrained minimization using the method of feasible directions search algorithm. Figure 3 is a flow chart of the optimization procedure. The procedure begins with the selection of an initial set of design variables. An analysis module performs the necessary thermal/structural analyses and the optimizer then calculates the objective function, constraints, and the gradients of the objective function and constraints with respect to design variables. Gradients required by the search algorithm are calculated by finite differences. Using the method of feasible directions search algorithm, the optimizer selects a search direction and minimizes the objective function in this direction. The design variables are modified to reflect this design choice and the procedure is repeated until one of several termination criteria is satisfied. The termination criteria are: (1) the percentage change in the objective function is less than some specified value, (2) there are three consecutive iterations without a change in the design variables, or (3) a feasible direction is not found after 10 iterations.

Design of Cylindrical Heat Pipes Embedded in a Honeycomb Core

The cylindrical heat pipes embedded in the honeycomb core (fig. 6) were minimized with respect to mass, and the corrugations or channels were sized, using the previously described procedures, subject to three heat transport constraints (sonic, entrainment, and axial wicking limits) (see appendix A, eqs. (A1) to (A3)). The design variables are the inner and outer radii of the channels (r_1 and r_2, respectively) and the width of the grooves W. The heat pipes were first optimized assuming that the coolant manifolds were located at either end of the panel (20 ft apart). The panels were then optimized for a variable number of equally spaced manifolds N_m, which accounted for the additional mass associated with

each manifold (0.065 lbm/ft^2 (ref. 7)). The working fluid chosen is toluene, and its properties at 300°F were obtained from reference 12. Hence, the three design variables for this problem are: $X_1 = r_1$, $X_2 = r_2$, and $X_3 = W$. The heat-pipe, heat-transport constraints (eqs. (A1) to (A3)) are related to the design variables through the cross-sectional areas, A_v and A_ℓ, and through the expression for wick permeability. The resulting expressions for objective function and constraints are as follows:

$$F(X) = \frac{(\rho_\ell A_\ell + \rho_s A_s + \rho_w A_w)(\text{No. of heat pipes})L + M}{bL}$$

$$g_1(X) = (r_1/r_2) - 1.0 \qquad \text{(geometric constraints)}$$

$$g_2(X) = 2(r_2 + 0.02) - 1.0$$

$$g_3(X) = \text{FS}(Q_{IN}/Q_{AW}) - 1.0 \quad \text{(wicking limit)}$$

$$g_4(X) = \text{FS}(Q_{IN}/Q_{AE}) - 1.0 \quad \text{(entrainment limit)}$$

$$g_5(X) = \text{FS}(Q_{IN}/Q_{AS}) - 1.0 \quad \text{(sonic limit)}$$

Upper and lower dimensional bounds (in inches) were also imposed as follows:

$$0.05 \le r_1 \le 1.0$$

$$0.05 \le r_2 \le 1.0$$

$$0.005 \le W \le 0.25$$

No constraint was imposed to ensure an integer number of grooves; hence, one of the grooves could be nonstandard in shape. The limits Q_{AW}, Q_{AS}, and Q_{AE} were calculated using equations (A1) to (A3) with

$$A_v = \pi r_2^2$$

$$A_\ell = \pi(r_2^2 - r_1^2)/2$$

$$A_s = \pi\left[(r_2 + 0.02)^2 - r_2^2\right] + \frac{(r_2^2 - r_1^2)}{2}$$

for the axial-grooved design and

$$A_\ell = \pi(r_2^2 - r_1^2)$$

$$A_s = \pi\left[(r_2 + 0.02)^2 - r_2^2\right]$$

for the corrugated composite screen wick. The permeability K_w is calculated for both wick designs as

$$K_w = \frac{2D^2W^2}{(D+W)^2}\left[-12.956(D/W)^3 + 33.605(D/W)^2 - 30.249(D/W) + 24.0\right]$$

where this expression represents a third-order curve fit of data presented in reference 13 and where $D = r_2 - r_1$.

The heat input to a single heat pipe and the effective heat-pipe length are

$$Q_{IN} = (\dot{q}_{\text{abs}} b L_{\text{eff}}) \frac{1}{\text{No. of heat pipes}}$$

and

$$L_{\text{eff}} = L/[2(N_m + 1)]$$

where L is the length of the panel (20 ft), $\dot{q}_{\text{abs}}$ is the net heat absorbed by the panel per unit area (0.8 Btu/ft^2-sec), and N_m is the number of additional manifolds.

Design of Heat-Pipe Web-Core Sandwich Panel

The heat-pipe web-core sandwich panel design (fig. 7) has a total of seven design variables. The design variables are the thickness of the face sheets t_f, the height of the core h_c, the web spacing S, the thickness of the core web t_c, the thickness of the composite wick along the web walls t_w, the depth of the channels D, and the width of the channels W. Hence, for this problem, the design variables are as follows: $X_1 = t_f$, $X_2 = t_c$, $X_3 = h_c$, $X_4 = S$, $X_5 = t_w$, $X_6 = D$, and $X_7 = W$. The constraints include axial (wicking, entrainment, and sonic limits) and transverse (wicking limit through the depth of the panel) heat-pipe constraints and strength, buckling, fatigue, and minimum-gage constraints. The objective function to be minimized is the panel mass per unit planform area. The effect of additional coolant manifolds is also investigated. The steady-state, heat-pipe-limit equations are similar to equations (A1) to (A3) of appendix A, with appropriate changes for A_ℓ, A_v, etc. A transverse wicking limit (through the depth of the panel) was also included in the analysis of the web-core design to ensure adequate liquid flow from the cooled to the heated face of the panel in the evaporator region (i.e., between the coolant manifolds). This amounts to a total of four heat-pipe constraints (three axial and one transverse).

In the structural analysis, it is assumed that the panel behaves as an orthotropic panel with panel stiffnesses calculated as functions of the design variables using references 14 and 15. Details of the strength, buckling, and fatigue analyses are presented in appendix B. The expression for the objective function is given by the following equation:

$$F(X) = \frac{(\rho_\ell A_\ell + \rho_s A_s + \rho_w A_w)(\text{No. of heat pipes})L + M}{bL}$$

The expressions for the normalized constraints are as follows:

$g_1(X) = \text{FS}(Q_{AIN}/Q_{AW}) - 1.0$ (axial wicking limit)

$g_2(X) = \text{FS}(Q_{AIN}/Q_{AE}) - 1.0$ (axial entrainment limit)

$g_3(X) = \text{FS}(Q_{AIN}/Q_{AS}) - 1.0$ (axial sonic limit)

$g_4(X) = \text{FS}(Q_{TIN}/Q_{TW}) - 1.0$ (transverse wicking limit)

$g_5(X) = \text{FS}(W/D) - 1.0$ (groove geometry constraint)

$g_6(X) = \text{FS}((t_c + 2t_w)/S) - 1.0$ (wick thickness constraint)

$g_7(X) = \text{FS}(\sigma_{x,f}/\sigma_{\text{ult}}) - 1.0$ (ultimate strength of faces)

$g_8(X) = \text{FS}(\tau_{zx,\max}/\tau_{\text{ult}}) - 1.0$ (shear strength of core)

$g_9(X) = \text{FS}(\sigma_{tc}/\sigma_{\text{ult}}) - 1.0$ (tensile strength of core)

$g_{10}(X) = \text{FS}(P_x/P_{x,ob}) - 1.0$ (overall panel buckling)

$g_{11}(X) = \text{FS}((\sigma_{x,\max} + P_x b/A_s)\sigma_{x,lb}) - 1.0$ (local buckling of faces)

$g_{12}(X) = \text{FS}(P_x b/A_s)/\sigma_{x,lb} - 1.0$ (local buckling of webs)

$g_{13}(X) = (\text{FS}(\sigma_{x,p})_f/\sigma_{\text{ult}}) - 1.0$ (burst failure of faces in x-direction)

$g_{14}(X) = (\text{FS}(\sigma_{y,p})_f/\sigma_{\text{ult}}) - 1.0$ (burst failure of faces in y-direction)

$g_{15}(X) = (\text{FS}(\sigma_{x,p})_c/\sigma_{\text{ult}}) - 1.0$ (burst failure of core in x-direction)

$g_{16}(X) = (\text{FS}(\sigma_{y,p})_c/\sigma_{\text{ult}}) - 1.0$ (burst failure of core in y-direction)

$g_{17}(X) = (\sigma_{x,\max} + P_x/A_s)\sigma_{x,\text{FAT}} - 1.0$ (fatigue failure of faces)

where

$$Q_{AIN} = Q_{IN}$$

and

$$Q_{TIN} = \dot{q}_{\text{abs}}(SL_{\text{eff}})$$

Upper and lower dimensional bounds (in inches) were also imposed as follows:

$0.01 \le t_f \le 1.0$
$0.01 \le t_c \le 1.0$
$0.125 \le h_c \le 10.0$
$0.25 \le S \le 2.0$
$0.005 \le t_w \le 0.25$
$0.005 \le D \le 0.25$
$0.005 \le W \le 0.25$

Results and Discussion

Cylindrical Heat Pipes Embedded in a Honeycomb Core

Results for the optimization of cylindrical heat pipes embedded in a honeycomb core are summarized in table 1. The optimization problem can be easily solved directly by noting that g_3 is the only constraint that is a function of W via the expression for K_w. The optimum dimensions of the groove which minimize fluid flow resistance occur when $W = r_2 - r_1$ (ref. 13); hence, the problem can be reduced to two dimensions or design variables if the wicking limit is a governing condition of the design, which it happens to be for this problem. This is a valid assumption, since the optimum design occurs at the intersection of several constraint boundaries, which for this problem are the entrainment-limit and the wicking-limit boundaries. Contours of constant values of the objective function F (which for this problem is only the mass of the heat pipes) and constraint boundaries are plotted as a function of the design variables r_1 and r_2 in figure 8. The feasible design space, with all constraints satisfied ($g_i \le 0$), is marked by the shaded region. It is bounded by g_2 (a geometric constraint on the outer diameter of the heat pipe), g_3 (the wicking limit), and g_4 (the entrainment limit). The sonic limit is not a limit on the feasible design space. (If plotted, the sonic-limit boundary would be a vertical line located at $r_1 = 0.07$ in.) Contours of constant objective function values are shown with the direction of increasing magnitude indicated. The optimum design point indicated in figure 8 occurs at the intersection of the entrainment- and wicking-limit curves. This closed-form solution corresponds to $r_1 = 0.275$ in., $r_2 = 0.343$ in., $W = 0.068$ in., and $F = 0.0145$ lbm/in^2. The problem was also solved using formal optimization methods and allowing W to be a free variable. The results after nine design iteration cycles from an initial infeasible design of $r_1 = 0.1$ in., $r_2 = 0.2$ in., and $W = 0.025$ in. are $r_1 = 0.277$ in., $r_2 = 0.359$ in., $W = 0.0711$ in., and $F = 0.0149$ lbm/in^2. The total HPCP mass was 0.033 lbm/in^2 after the face sheets were resized for structural constraints. The total panel mass (ref. 7) includes the heat-pipe mass and two manifolds (0.065 lbm/ft^2 each) but does not include the radiation system (1.49 lbm/ft^2), panel coolant (0.12 lbm/ft^2), D-tube (0.16 lbm/ft^2), and difference in resized face-sheet masses. This mass compares with an

ACP mass of 0.02104 lbm/in^2 from reference 7 (total RACP panel mass not considering the radiation system). The iteration history of the formal optimization procedure is shown in figure 8 by the arrows. The starting design is infeasible (violates constraints 3 and 4); however, the process moves into the feasible region after three iterations and satisfies the first termination criterion after nine iterations (less than 0.1-percent change in the objective function). Results from the direct solution and the formal optimization solution agree well with slight discrepancies caused by the approximate nature of the expression for K_w and by the fact that $W \neq r_2 - r_1$. If an additional constraint were included in the formal optimization such that $W = r_2 - r_1$, the results would agree exactly with the direct solution. The simplicity of this problem enables a graphical solution for comparison; for practical design studies, where the number of design variables and constraints is large, an exact solution is not possible. Plots of the objective-function, design-variable, and constraint iteration histories are shown in figures 9 to 11. As shown in figures 9 and 11, the initial design is infeasible with a low mass. The mass increases as the design moves toward the feasible design space and reaches a maximum after two cycles (fig. 9). Figure 10 shows the iteration history of the design variables; the design variables converge after eight iterations. Designs are in the feasible design space after three iterations (fig. 11) and remain feasible, with minor excursions, throughout the remainder of the optimization history. The design process proceeds in the feasible region and minimizes the mass as previously shown in figure 8. This procedure was repeated for increasing numbers of additional manifolds and for the corrugated-screen composite wick design, and the results are presented in figure 12. A minimum-mass, axial-grooved, heat-pipe panel (0.0092 lbm/in^2) results for five equally spaced additional coolant manifolds (3⅓ ft apart); this amounts to a total panel mass of 0.0284 lbm/in^2, compared with 0.033 lbm/in^2 if there are no additional manifolds. Results for the corrugated-screen design indicate a total HPCP panel mass of 0.0283 lbm/in^2 with no additional manifolds and a minimum mass of 0.0276 lbm/in^2 with two additional manifolds.

Heat-Pipe Web-Core Sandwich Panel

Results for the screen-covered, grooved-wick design (fig. 7(a)), starting from an initial design listed in table 2, indicate that with no additional manifolds a minimum cooled-panel mass of 0.0279 lbm/in^2 results.

The total HPCP mass is the sum of the total ACP mass of reference 7 (4.52 lbm/ft^2) and the heat-pipe web-core panel mass with any additional coolant manifolds (0.065 lbm/ft^2 each) minus the face sheets (1.20 lbm/ft^2), D-tubes (0.16 lbm/ft^2), honeycomb (0.29 lbm/ft^2), radiation system (1.49 lbm/ft^2), panel coolant mass (0.12 lbm/ft^2), and adhesive (0.4 lbm/ft^2). A minimum mass of 0.0221 lbm/in^2 is achieved by adding three additional manifolds. Results for the corrugated-screen composite wick also listed in table 2 indicate that with no additional manifolds, a minimum structural panel mass of 0.0161 lbm/in^2 results, which corresponds to a total HPCP panel mass of 0.0221 lbm/in^2. The optimum design with respect to additional manifolds is 0.0157 lbm/in^2 with one additional manifold and corresponds to a total HPCP panel mass of 0.0216 lbm/in^2. Again, this is compared with an ACP panel mass (ref. 7) of 0.02104 lbm/in^2 (total RACP panel mass excluding the radiation system).

Iteration histories for a typical optimization are shown in figures 13 to 15 for a corrugated-composite screen wick design with no additional manifolds. The variable histories (fig. 14) were all normalized to their initial dimensions. Convergence to a local minimum occurs after 18 iterations. The initial starting design is infeasible (violates axial-wicking and local web-buckling constraints g_1 and g_{12}, respectively, fig. 15). A feasible design is reached after two iterations ($F = 0.0174$ lbm/in^2), and panel mass is reduced to a minimum value of $F = 0.016$ lbm/in^2 after 18 iterations (fig. 13).

The individual CPU times needed to achieve the minimum HPCP designs using formal optimization methods are about 1 minute with a CDC® Cyber 173 computer. Hence, if new designs are required because of changes in loading conditions, constraints, etc., optimum configurations can be determined quickly. Although formal optimization techniques may appear to be useful in a black-box mode, it is necessary for someone familiar with each aspect of the engineering design to monitor results of the optimization process. Such engineering experience is necessary to make critical decisions when problems arise in the optimization because of

1. a failure to satisfy specific constraints and produce a feasible design
2. a failure to include a relevant design constraint
3. inadequate analysis methods based on changes which occur during the design
4. any number of other scenarios which might produce a design which does not appear to be realistic

Concluding Remarks

Results of this study indicate that formal optimization methods can be used to design heat-pipe systems to perform several functions efficiently. Several structurally efficient heat-pipe panels were designed and optimized with respect to mass and subjected to heat-transport, strength, buckling, fatigue, and minimum-gage constraints. Optimum panel designs were also obtained for various numbers of additional coolant manifolds where the thermal but not structural effect of additional manifolds was considered. A nonintegrated design—cylindrical heat pipes embedded in a honeycomb sandwich—with three design variables and five constraints, was optimized using an optimizer, CONMIN, for constrained function minimization. Optimum panel masses for a screen-covered, axial-grooved wick design were 0.033 lbm/in^2 with no additional manifolds and 0.0284 lbm/in^2 with five additional manifolds. For the corrugated-screen wick design, the optimum panel masses were 0.0283 and 0.0276 lbm/in^2 with no additional manifolds and two additional manifolds, respectively. The accuracy of the optimum results using CONMIN was checked with a closed-form solution for the cylindrical heat pipe, and results agree well. Results for an integrated design—heat-pipe web-core sandwich panel—were consistently lighter than for the discrete tube design (heat pipes embedded in honeycomb sandwich) by approximately 20 percent. Results for screen-covered, grooved-face-sheets wick design were 0.0279 and 0.0221 lbm/in^2 with no additional manifolds and three additional manifolds, respectively. Results for a corrugated-composite-screen wick design were 0.022 and 0.0216 lbm/in^2 with no additional manifolds and one additional manifold, respectively. The web-core panel design had a total of 7 design variables and 17 constraints; hence, formal optimization methods were necessary to find a minimum-mass design. Feasible designs were found after several design iterations, and minimum-mass designs were reached in about 20 iterations and required about 1 minute of CPU time on a CDC® Cyber 173 computer.

The study also verified the feasibility of using heat pipes in conjunction with active cooling to cool the structure of hypersonic cruise aircraft. The resulting designs offer a mass-competitive alternative to a redundant, completely actively cooled design.

NASA Langley Research Center
Hampton, Virginia 23665-5225
August 14, 1987

Appendix A
Heat-Pipe Operational Limits

Heat-pipe operation is analyzed assuming steady-state, one-dimensional, incompressible, laminar fluid flow with complete pressure recovery in the vapor region. Liquid flow in the wick is described by Darcy's law, and a constant heat flux is assumed over the panel surface. Three fluid-dynamic heat-transfer limits, the wicking limit (capillary pumping limit), the entrainment limit, and the sonic limit, were considered in the present analysis.

Wicking Limit

The wicking limit is the heat-transport limit that occurs when the capillary pumping action of the wick is just sufficient to balance the gravitational pressure head of the liquid and the inertial and frictional losses of the fluid. The expressions for the wicking limit are obtained as follows using the method of reference 16:

$$Q_{AW} = 2\sigma_\ell / \left\{ r_p \left[(\mu_v L_{\text{eff}} / g_c A_\ell K_w \lambda \rho_\ell) + (8\mu_\ell L_{\text{eff}} / g_c \pi r_v^4 \rho_v \lambda) \right] \right\} \qquad \text{(A1)}$$

where σ_ℓ is the liquid surface tension, ρ_v and ρ_ℓ are the vapor and liquid mass densities, r_p is the pore radius of the wick, A_ℓ is the liquid-flow cross-sectional area, λ is the latent heat of vaporization of the working fluid, r_v is the hydraulic radius of the vapor space, L_{eff} is the effective length of the heat pipe, μ_v and μ_ℓ are the vapor and liquid viscosities, K_w is the permeability of the wick, and g_c is the gravitational constant. Since coolant manifolds are located at either end of the panel, it is assumed that the effect of vehicle acceleration forces can be neglected.

Entrainment Limit

The entrainment limit occurs when the vapor velocity is large enough so that the drag force exerted on the returning liquid condensate overcomes the surface-tension forces of the liquid and liquid droplets are entrained in the vapor space and swept away in the opposite direction. This causes liquid depletion in the heated area and the eventual drying out of the heat pipe. The entrainment limit is assumed to occur when the Weber number (ratio of inertial vapor force to liquid surface-tension force) is equal to unity. The entrainment limit is expressed as

$$Q_{AE} = A_v \left(g_c \rho_v \sigma_\ell \lambda^2 / 2 r_p \right)^{1/2} \qquad \text{(A2)}$$

Sonic Limit

The sonic limit occurs when the vapor flow velocity reaches a sonic condition. The heat transported is thus limited by this choked flow condition and is expressed as

$$Q_{AS} = \frac{A_v p_v \lambda a_o}{\sqrt{2(1+\gamma)}} \qquad \text{(A3)}$$

where A_v is the cross-sectional area of the vapor space, p_v is the vapor pressure, γ is the ratio of specific heats, and a_o is the sonic velocity of the vapor.

Appendix B

Structural Analysis of Heat-Pipe Web-Core Sandwich Panel

In the structural analysis the panel is assumed to behave as an orthotropic panel with stiffness properties calculated as functions of the design variables using references 14 and 15. Equations derived in reference 17 are used to calculate maximum bending moment and shear load for a simply supported panel (2 ft × 2 ft, dimensions of panel between rings and stiffeners) subject to in-plane and uniform transverse loads as shown below:

$$M_{x,\max} - qb^2\beta_2 \tag{B1}$$

$$Q_{x,\max} - qb\beta_5 \tag{B2}$$

where β_2 and β_5 are functions of all the design variables shown in figure 7 except t_w (ref. 17), where q is the applied uniform transverse load, and where b is the width of the panel. The panel bending stress is then calculated using simple beam theory as

$$\sigma_{x,\max} = M_{x,\max} y / I_x \tag{B3}$$

where y is the distance from the neutral axis of the panel to the midplane of the faces ($y = (t_f + h_c/2)$) and where I_x is the moment of inertia of the panel about the neutral axis per unit panel width. The maximum shear stress $\tau_{zx,\max}$ is calculated from reference 17 to occur at the center of the core and is

$$\tau_{zx,\max} = VQ_{x,\max}/(2I_x t_c) \tag{B4}$$

where V is the static moment of the cross-sectional area above the neutral axis.

The effect of internal pressure ($p_v = 39.9$ psi for toluene at 300°F) was included using reference 18 and assuming that the face sheets and core web (fig. 7) act as simply supported plates. The expressions for stresses in the plates are

$$\sigma_{x,p} = \left\{6p_v / \left[\pi^2 t^2 \left(1/\ell^2 + 1/w^2\right)^2\right]\right\}\left(1/\ell^2 + \upsilon/w^2\right) \tag{B5}$$

$$\sigma_{y,p} = \left\{6p_v / \left[\pi^2 t^2 \left(1/\ell^2 + 1/w^2\right)^2\right]\right\}\left(\upsilon/\ell^2 + 1/w^2\right) \tag{B6}$$

where the local width w (used in eqs. (B5) and (B6)) of the face-sheet plate is S, and the local width of the web plate is h_c. The local length ℓ is the length of the panel between rings (2 ft). The internal pressure is p_v, t is the plate thickness, ℓ and w are the length and width of the plate, respectively, and υ is Poisson's ratio. Hence, the axial stress in the faces of the plate is

$$\sigma_{x,f} = \sigma_{x,\max} + \sigma_{x,p} + P_x b/A_s \tag{B7}$$

where P_x is the applied in-plane load per unit width, A_s is the total cross-sectional area of the panel which sustains load, and b is the panel width. The faces and walls were also sized to withstand, without failure, a burst pressure of four times the actual internal pressure. The tensile stresses in the webs due to internal pressure are

$$\sigma_{tc} = p_v(S/t_c) \tag{B8}$$

Overall panel buckling load is calculated using the following equation from reference 17:

$$P_{x,ob} = \left(\Phi_o \pi^2 D_x\right) / \left[b^2\left(m^2 b^2/\ell^2\right)\right] \tag{B9}$$

where m is the number of half waves in the longitudinal direction and is varied to produce a minimum value of $P_{x,ob}$ for buckling, and where Φ_o is a buckling parameter defined in reference 17.

Local buckling of the face sheets and webs was calculated using reference 19, assuming simply supported plates, and results in

$$\sigma_{x,lb} = 3.29(t/w)^2[E/(1-\upsilon^2)] \tag{B10}$$

where t is the thickness of the plate and w is the plate width (S for face sheet and h_c for webs).

The panels were designed to sustain design limit loads without yielding and ultimate loads without failure. A modified Wheeler model was used for fatigue analysis, similar to that of reference 20, and material property values for aluminum alloy AL 2219-T81 were obtained from references 7 and 8. For values of the maximum stress ratio $R = -1$ ($R = f_{\min}/f_{\max}$), a stress-intensity factor $K_c = 105$ ksi-$\sqrt{\text{in.}}$, and an initial flaw size of 0.005 in., the following equation was used to predict crack growth:

$$da/dN = 3.8637 \times 10^{-6}(\Delta K)^{2.2044} / [(1-R)K_c - \Delta K] \tag{B11}$$

where

$$\Delta K = 1.12\left(f_{\max} - f_{\min}\right)\frac{\pi a}{Q} \tag{B12}$$

where a is the crack length, Q is the flaw shape parameter (ref. 20), and $f_{\max}$ and $f_{\min}$ are the maximum and minimum cyclic stresses, respectively.

Plots of cycles to failure versus stress for various face-sheet thicknesses were used to determine an allowable stress as a function of face-sheet thickness (based on 20 000 cycles to failure) to be used as the fatigue constraint. Interpolated values using a third-order curve fit results in the expression

$$\sigma_{x,\mathrm{FAT}} = 0.4608 \times 10^8 (t_f)^3 - 0.8906 \times 10^7 (t_f)^2 + 0.6363 \times 10^6 (t_f) + 0.082727 \times 10^3 \tag{B13}$$

for an allowable stress due to fatigue.

References

1. Schmit, Lucien A.: Structural Synthesis—Its Genesis and Development. *AIAA J.*, vol. 19, no. 10, Oct. 1981, pp. 1249–1263.
2. Ashley, Holt: On Making Things Best—Aeronautical Uses of Optimization. *J. Aircr.*, vol. 19, no. 1, Jan. 1982, pp. 5–28.
3. Filippi, F.; Nervegna, N.; and Zarotti, G. L.: Modularity and Optimization in Fluid Loop Radiator Systems. ASME Paper 79-ENAs-37, July 1979.
4. Wright, J. P.: Optimization of Large Heat Pipe Radiators for Long Life Space Heat Rejection Systems. ASME Paper 79-ENAs-25, July 1979.
5. Brown, Richard F.; and Alario, Joseph P.: Space Constructible Radiator System Optimization. SAE Tech. Paper Ser. 851324, July 1985.
6. Shore, Charles P.; Nowak, Robert J.; and Kelly, H. Neale: *Flightweight Radiantly and Actively Cooled Panel—Thermal and Structural Performance.* NASA TP-2074, 1982.
7. Ellis, D. A.; Pagel, L. L.; and Schaeffer, D. M.: *Design and Fabrication of a Radiative Actively Cooled Honeycomb Sandwich Structural Panel for a Hypersonic Aircraft.* NASA CR-2957, 1978.
8. Koch, L. C.; and Pagel, L. L.: *High Heat Flux Actively Cooled Honeycomb Sandwich Structural Panel for a Hypersonic Aircraft.* NASA CR-2959, 1978.
9. Vanderplaats, Garret N.: *CONMIN—A FORTRAN Program for Constrained Function Minimization– User's Manual.* NASA TM X-62282, 1973.
10. Riley, Kathleen M.: *FRANOPP—Framework for Analysis and Optimization Problems—User's Guide.* NASA CR-165653, 1981.
11. Tanzer, H. J.: *Fabrication and Development of Several Heat Pipe Honeycomb Sandwich Panel Concepts.* NASA CR-165962, 1982.
12. Thermophysical Properties of Heat Pipe Working Fluids: Operating Range Between −60°C and 300°C. Eng. Sci. Data Item No. 80017, Engineering Sciences Data Unit (London), Aug. 1980.
13. Dynatherm Corp.: *Heat Pipe Design Handbook, Part I.* NASA CR-134264, 1972.
14. Libove, Charles; and Hubka, Ralph E.: *Elastic Constants for Corrugated-Core Sandwich Plates.* NACA TN 2289, 1951.
15. Anderson, Melvin S.: *Optimum Proportions of Truss-Core and Web-Core Sandwich Plates Loaded in Compression.* NASA TN D-98, 1959.
16. Dunn, P.; and Reay, D. A.: *Heat Pipes.* Pergamon Press, c.1976.
17. Allen, Howard G.: *Analysis and Design of Structural Sandwich Panels.* Pergamon Press, Inc., c.1969.
18. Timoshenko, S.; and Woinowsky-Krieger, S.: *Theory of Plates and Shells, Second ed.* McGraw-Hill Book Co., Inc., 1959.
19. Roark, Raymond J.; and Young, Warren C.: *Formulas for Stress and Strain, Fifth ed.* McGraw-Hill Book Co., c.1975.
20. F-4 Aircraft Structural Integrity Team, McDonnell Aircraft Co.: *F4 Fatigue and Damage Tolerance Assessment Program, Volume I.* MDC A2883 (Contract no. AFSC F33657-73-A-0062), June 28, 1974. (Revised May 30, 1980.)

Table 1. Results of Cylindrical Heat Pipes Embedded in a Honeycomb Sandwich

Cylindrical heat pipes in honeycomb	Initial design, in.	Final design, in.	[1]Final cooled-panel mass, lbm/in^2	Additional manifolds
Screen-covered grooves	$r_1 = 0.2$ $r_2 = 0.3$ $W = 0.05$	$r_1 = 0.277$ $r_2 = 0.351$ $W = 0.0711$	0.033	0
	$r_1 = 0.2$ $r_2 = 0.3$ $W = 0.05$	$r_1 = 0.1665$ $r_2 = 0.2187$ $W = 0.0518$	0.0284	5
Corrugated-composite screen wick	$r_1 = 0.2$ $r_2 = 0.3$ $W = 0.05$	$r_1 = 0.2554$ $r_2 = 0.3222$ $W = 0.0668$	0.0283	0
	$r_1 = 0.2$ $r_2 = 0.3$ $W = 0.05$	$r_1 = 0.1722$ $r_2 = 0.2318$ $W = 0.0593$	0.0276	2

[1]Radiation system not included.

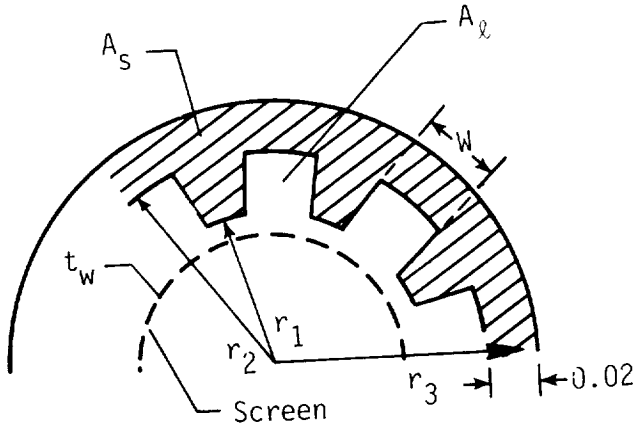

Design variables:
r_1, r_2, W

Table 2. Results of Web-Core Sandwich Panel

Heat-pipe web-core panel	Initial design, in.	Final design, in.	[1]Final cooled-panel mass, lbm/in^2	Additional manifolds
Screen-covered grooved face sheets	$t_f = 0.03$ $t_c = 0.02$ $h_c = 1.00$ $S = 0.50$ $t_w = 0.01$ $D = 0.05$ $W = 0.05$	$t_f = 0.0309$ $t_c = 0.0292$ $h_c = 0.7341$ $S = 0.6868$ $t_w = 0.0087$ $D = 0.0949$ $W = 0.0946$	0.0279	0
	$t_f = 0.03$ $t_c = 0.02$ $h_c = 1.00$ $S = 0.50$ $t_w = 0.01$ $D = 0.05$ $W = 0.05$	$t_f = 0.0317$ $t_c = 0.0293$ $h_c = 0.7333$ $S = 0.6883$ $t_w = 0.0099$ $D = 0.0345$ $W = 0.0345$	0.0221	3
Corrugated-composite wick	$t_f = 0.03$ $t_c = 0.02$ $h_c = 1.00$ $S = 0.50$ $t_w = 0.01$ $D = 0.05$ $W = 0.05$	$t_f = 0.0311$ $t_c = 0.0307$ $h_c = 0.8287$ $S = 0.6905$ $t_w = 0.0093$ $D = 0.0731$ $W = 0.0730$	0.022	0
	$t_f = 0.03$ $t_c = 0.02$ $h_c = 1.00$ $S = 0.50$ $t_w = 0.01$ $D = 0.05$ $W = 0.05$	$t_f = 0.03265$ $t_c = 0.02401$ $h_c = 0.6617$ $S = 0.4260$ $t_w = 0.0098$ $D = 0.0467$ $W = 0.0465$	0.0216	1

[1]Radiation system not included.

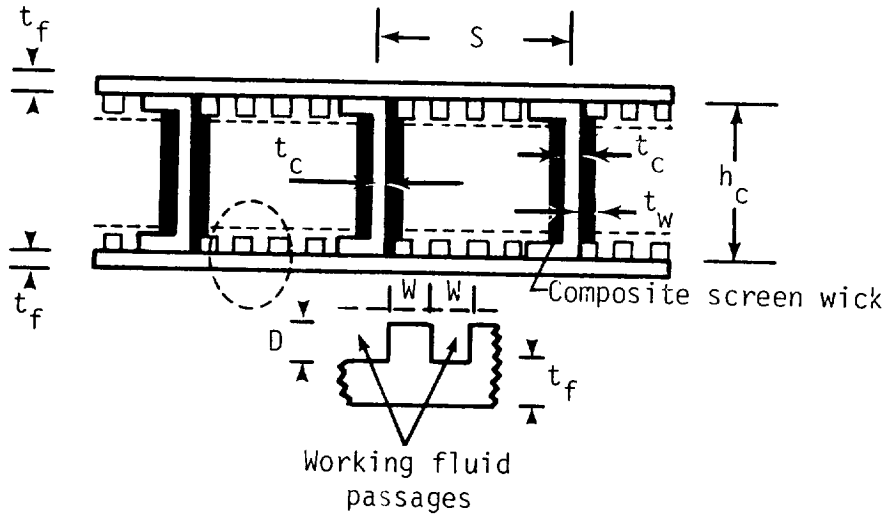

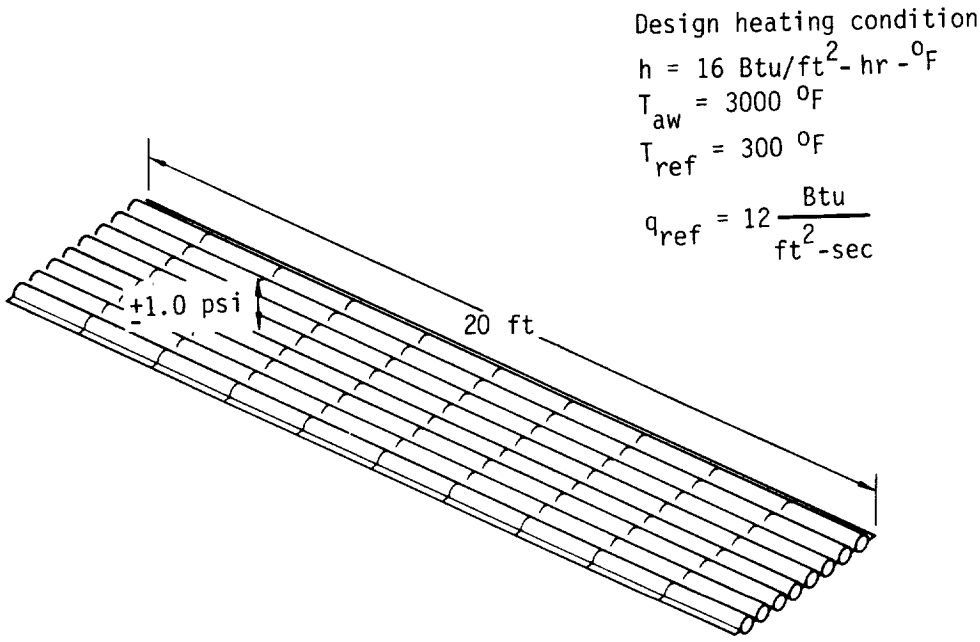

(a) Heat shield.

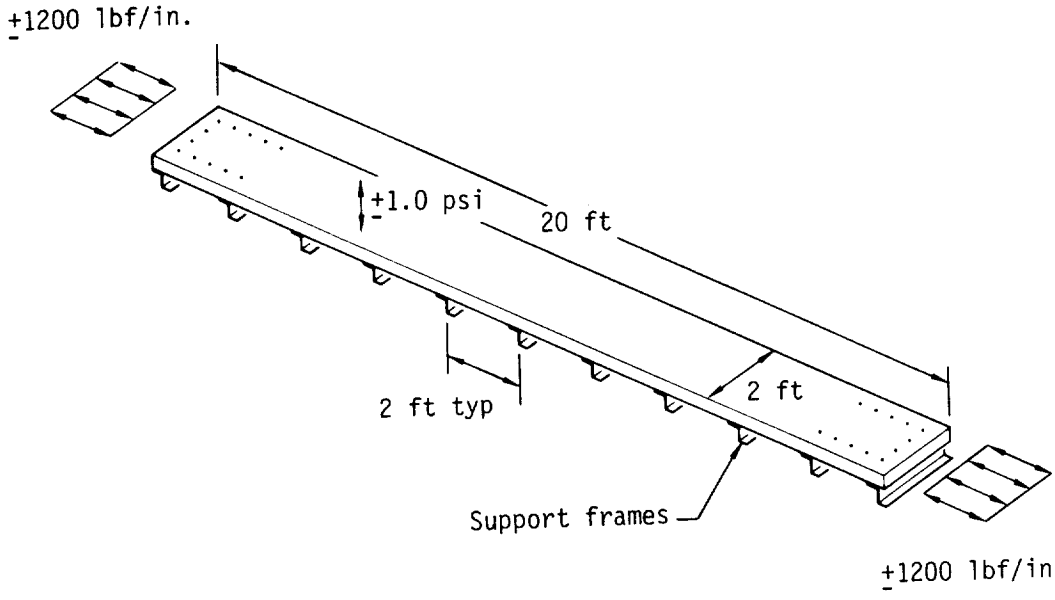

(b) Actively cooled panel.

Figure 1. Radiantly and actively cooled panel (RACP) design loads and heat flux.

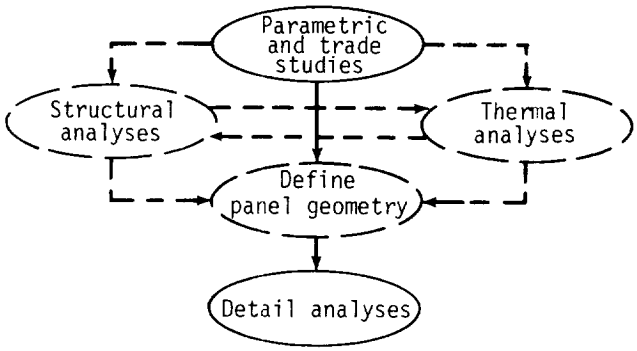

(a) Panel design sequence.

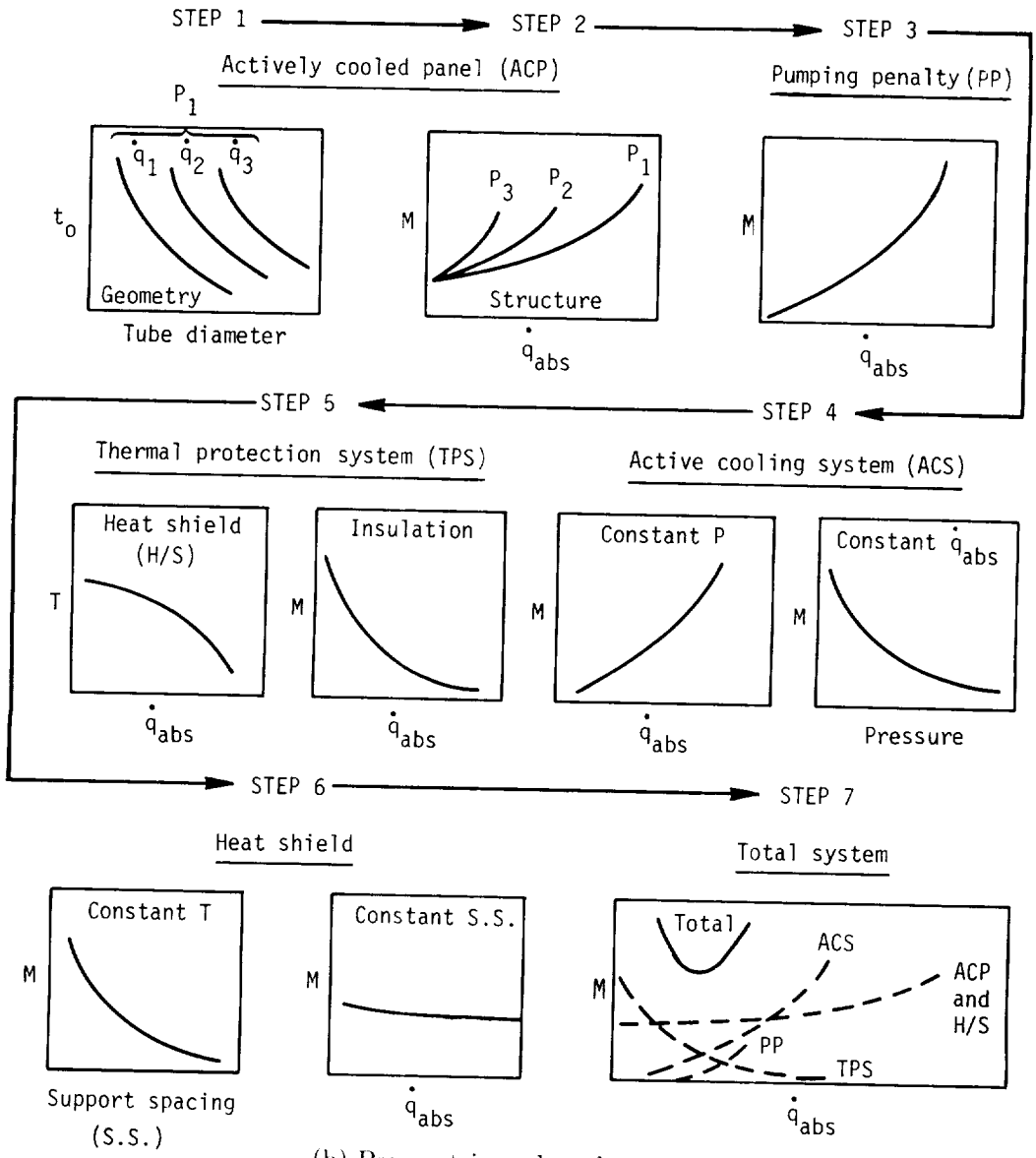

(b) Parametric and trade studies.

Figure 2. Design methodology used for radiantly and actively cooled panel (RACP (ref. 7)).

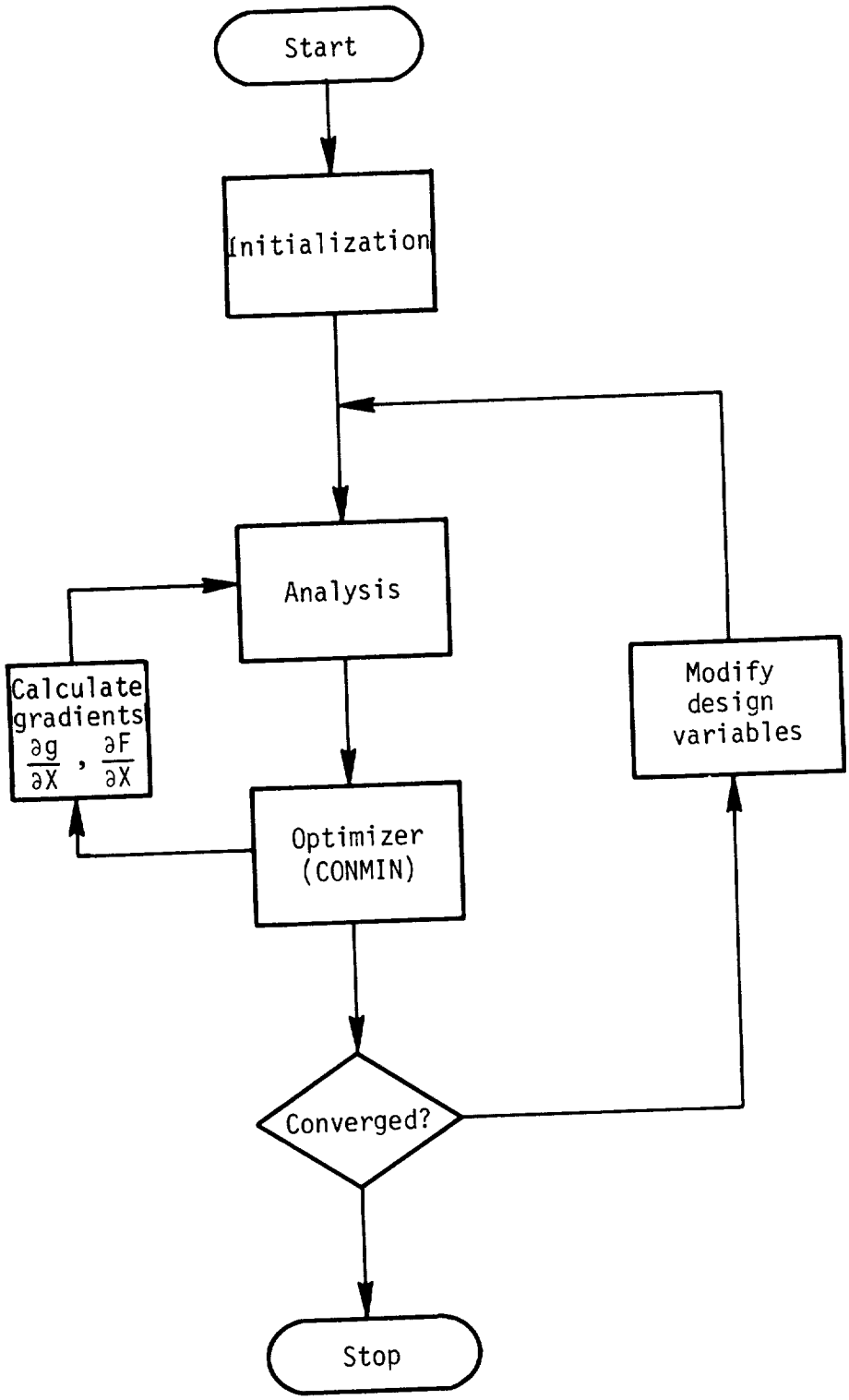

Figure 3. Flow chart of optimization procedure.

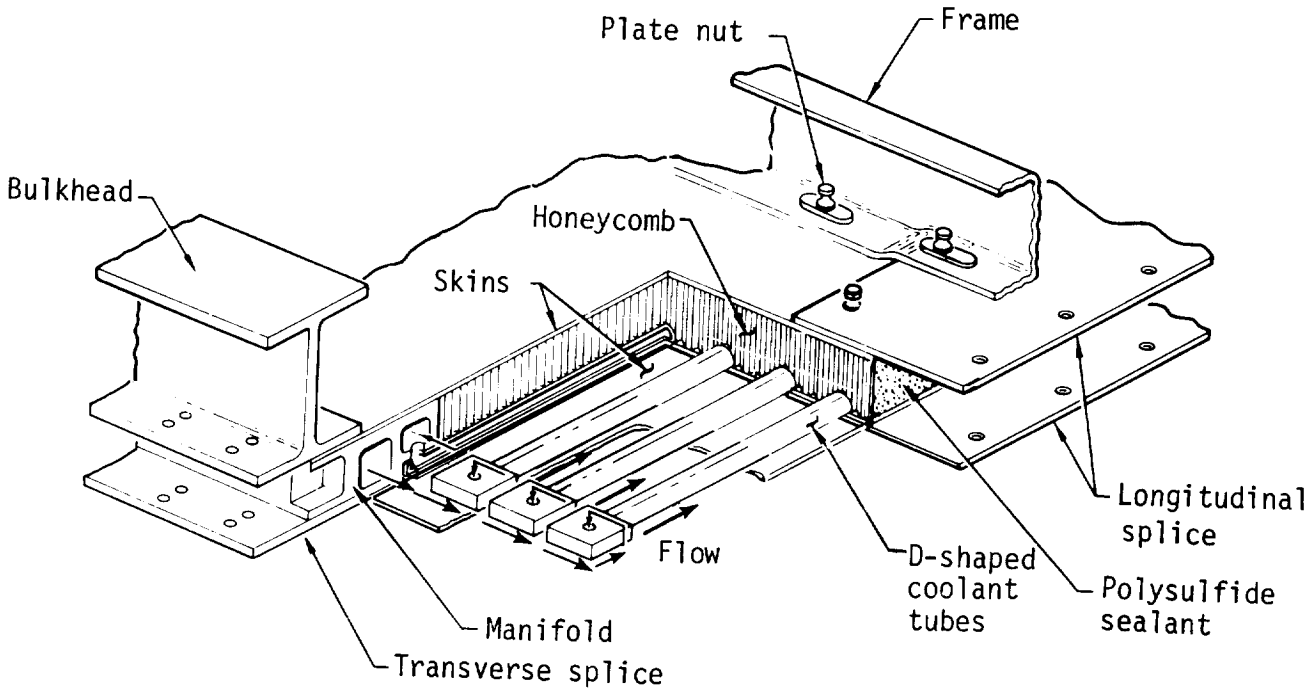

(a) Schematic of ACP.

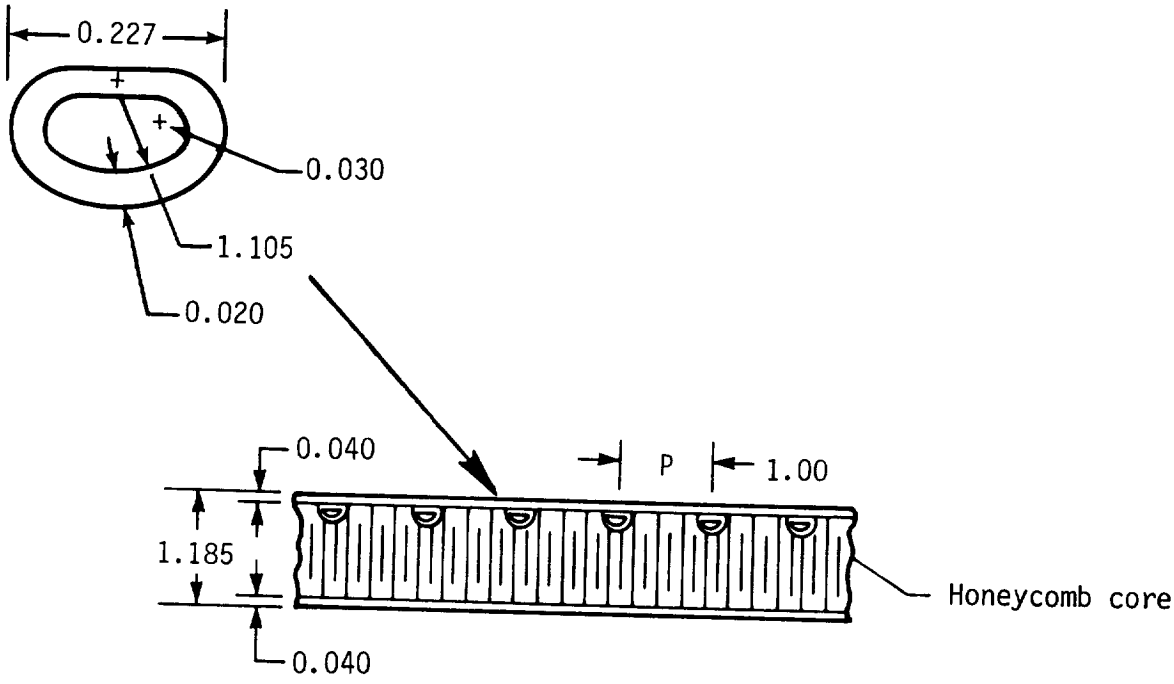

(b) Cross section of ACP.

Figure 4. Details of ACP. All dimensions in inches.

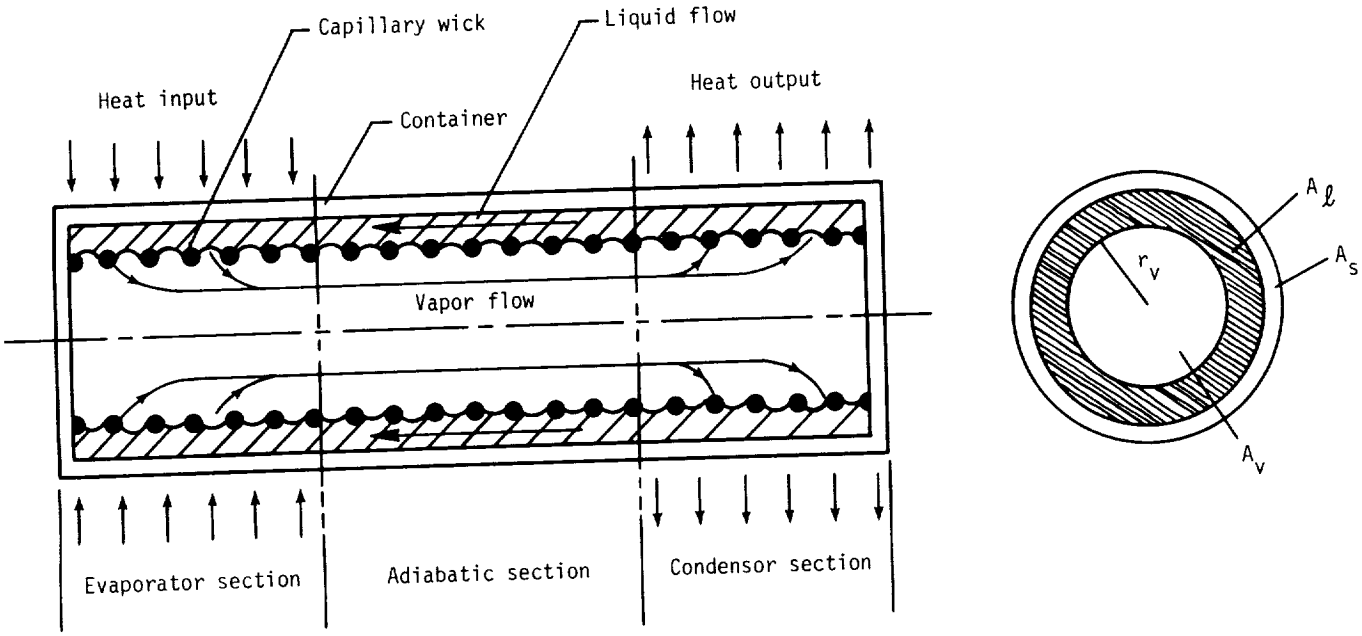

Figure 5. Schematic of heat-pipe operations.

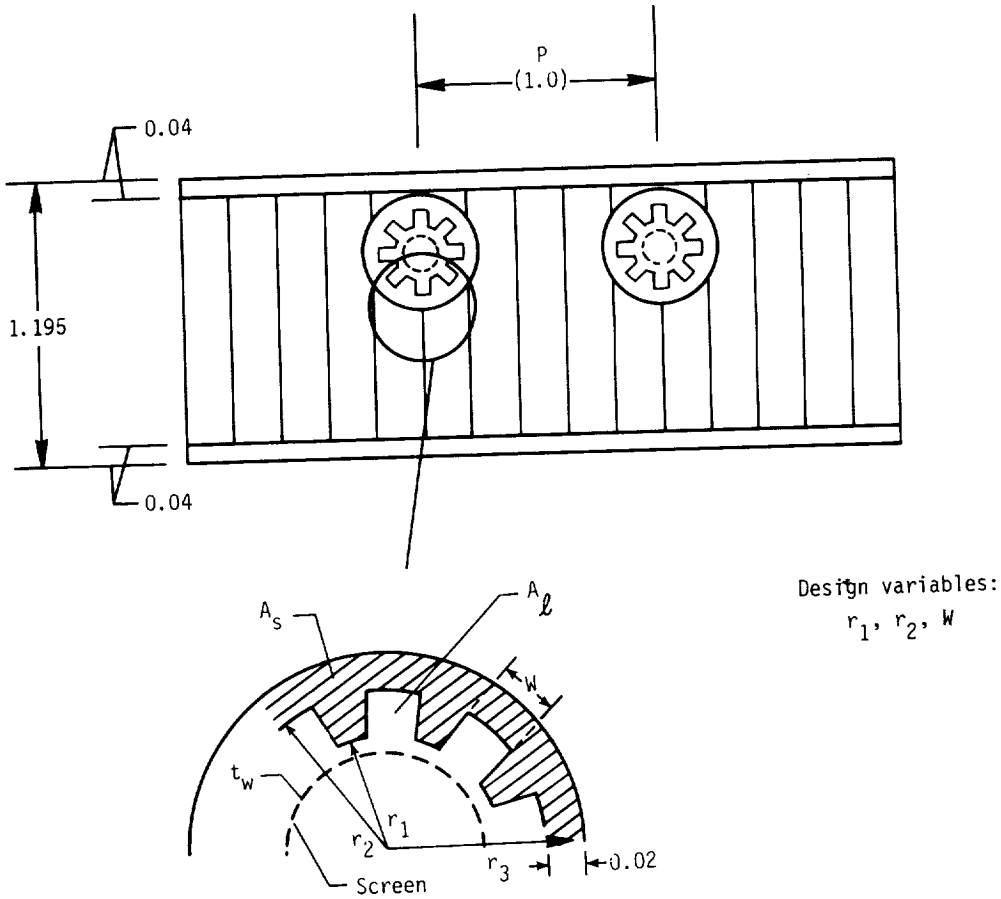

Figure 6. Heat pipes embedded in honeycomb sandwich. All dimensions in inches.

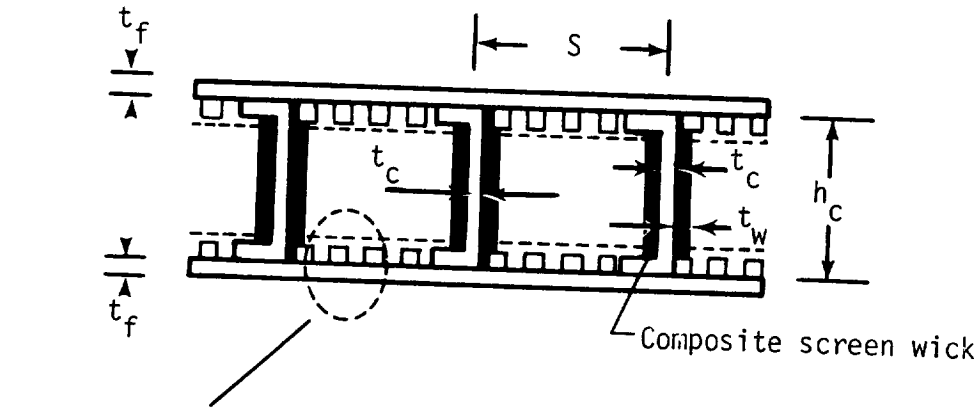

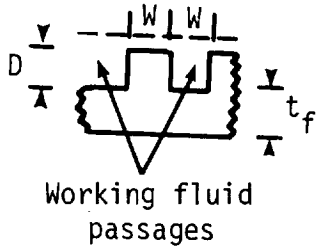

(a) Screen-covered axial grooves.

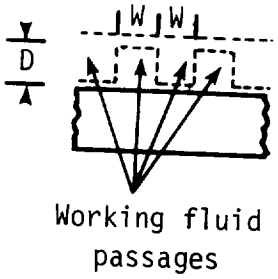

(b) Corrugated sandwich screen wick.

Design variables: t_f, t_c, h_c, S, t_w, D, W

Figure 7. Heat-pipe web-core sandwich panel designs.

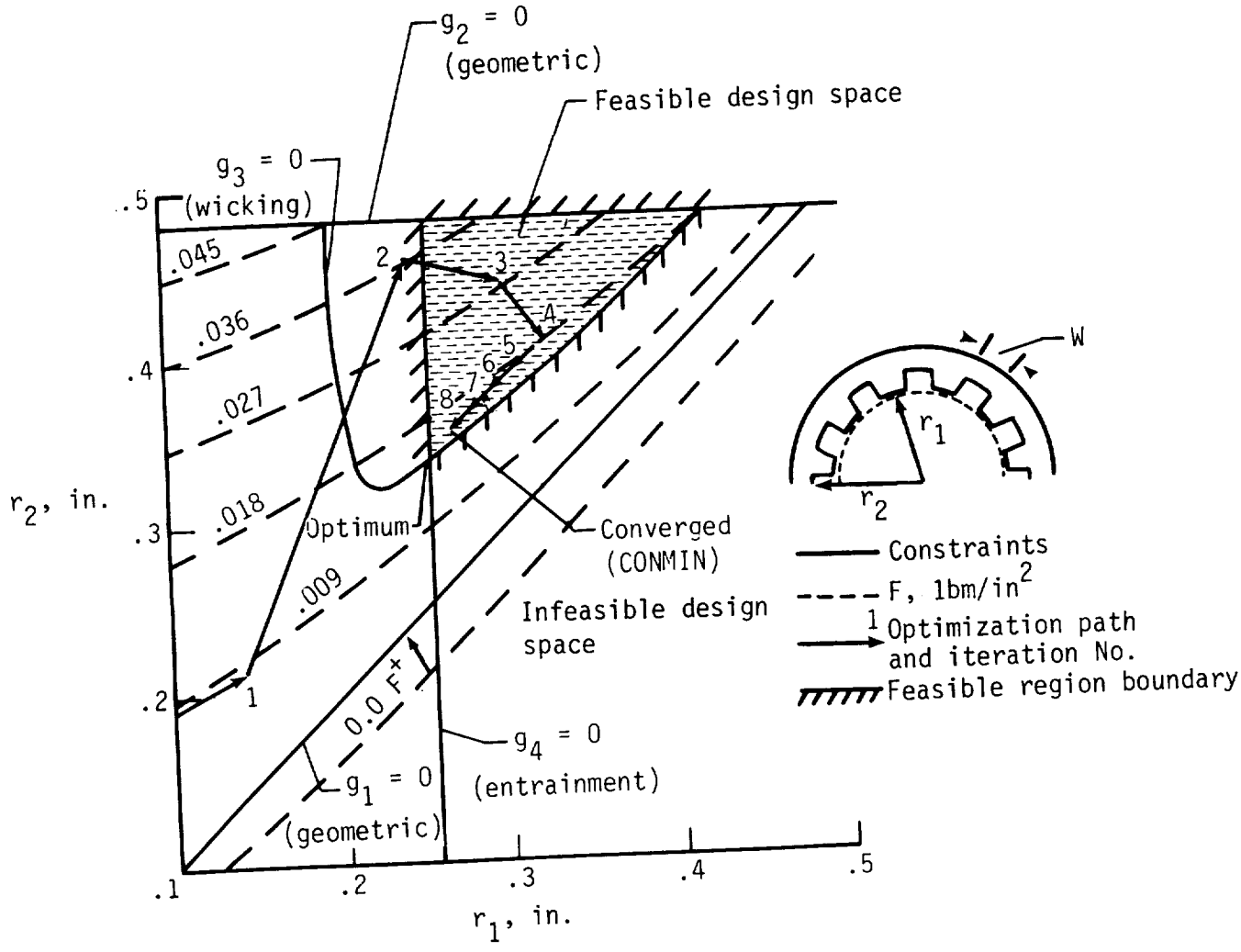

Figure 8. Optimum design of screen-covered axial-grooved heat pipe. $Q = 0.8$ Btu/ft^2-sec; $L = 20$ ft; $r_p = 0.0009055$ in.; working fluid is toluene.

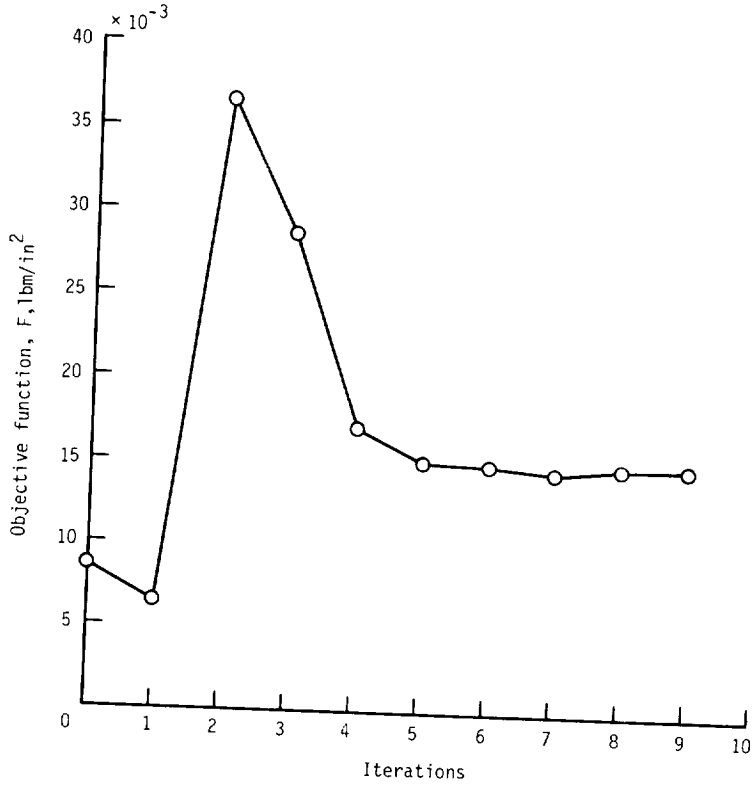

Figure 9. Objective function iteration history (axial-grooved heat pipe with no additional coolant manifolds).

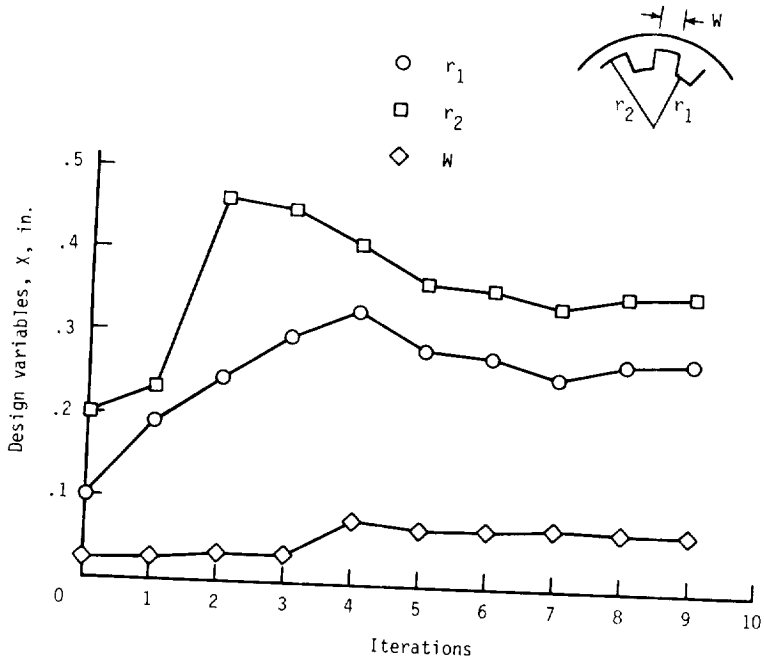

Figure 10. Design-variable iteration history (axial-grooved heat pipe with no additional coolant manifolds).

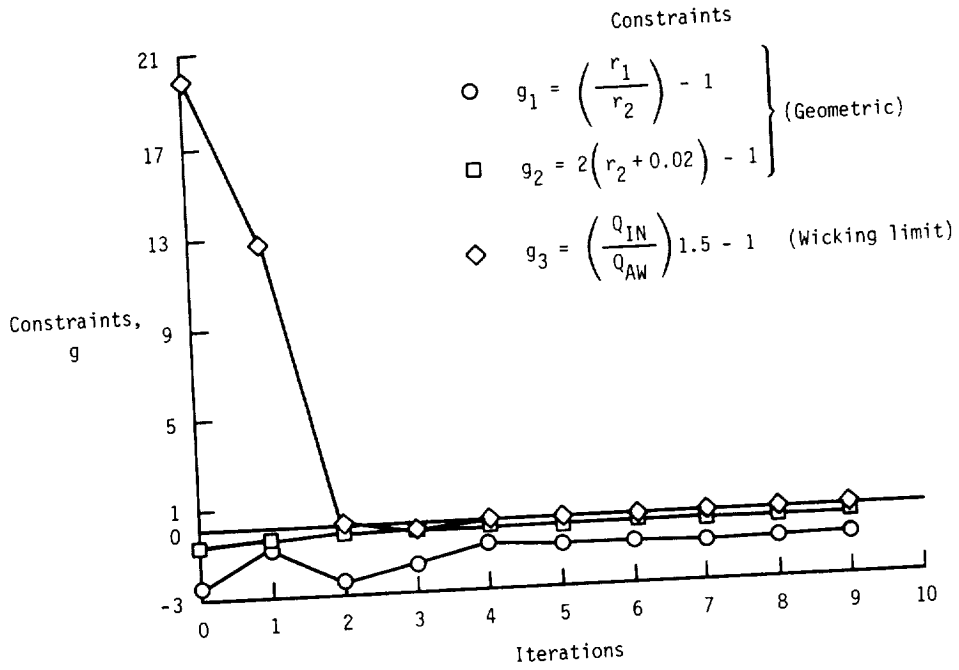

Figure 11. Constraint iteration histories (axial-grooved heat pipe with no additional coolant manifolds).

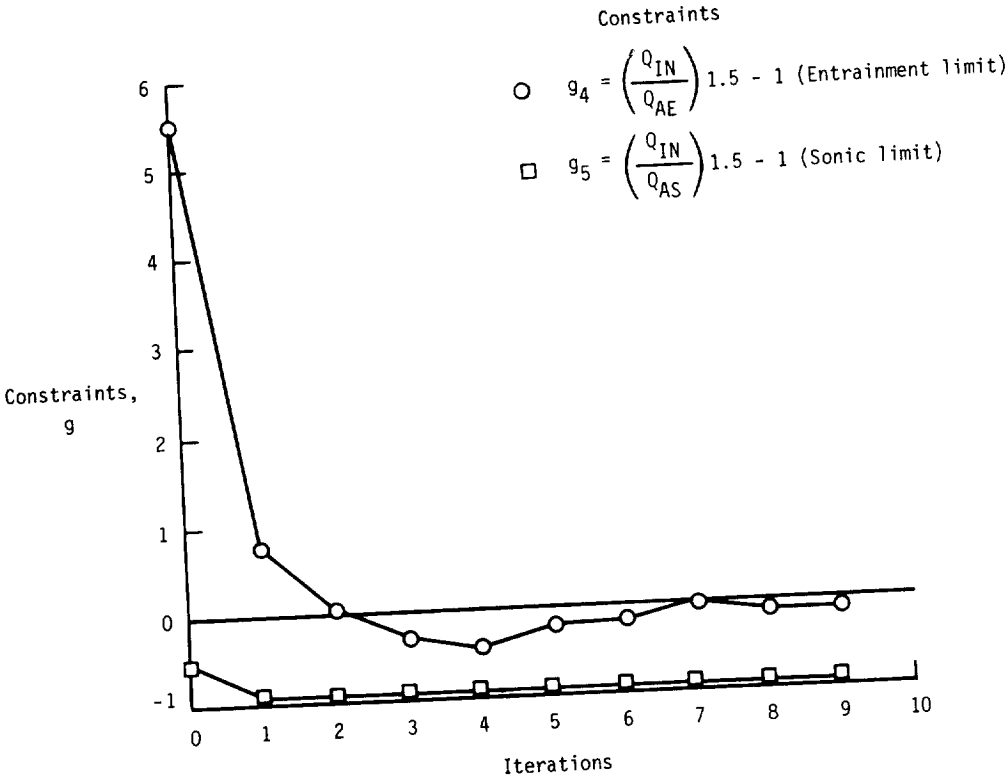

Figure 11. Concluded.

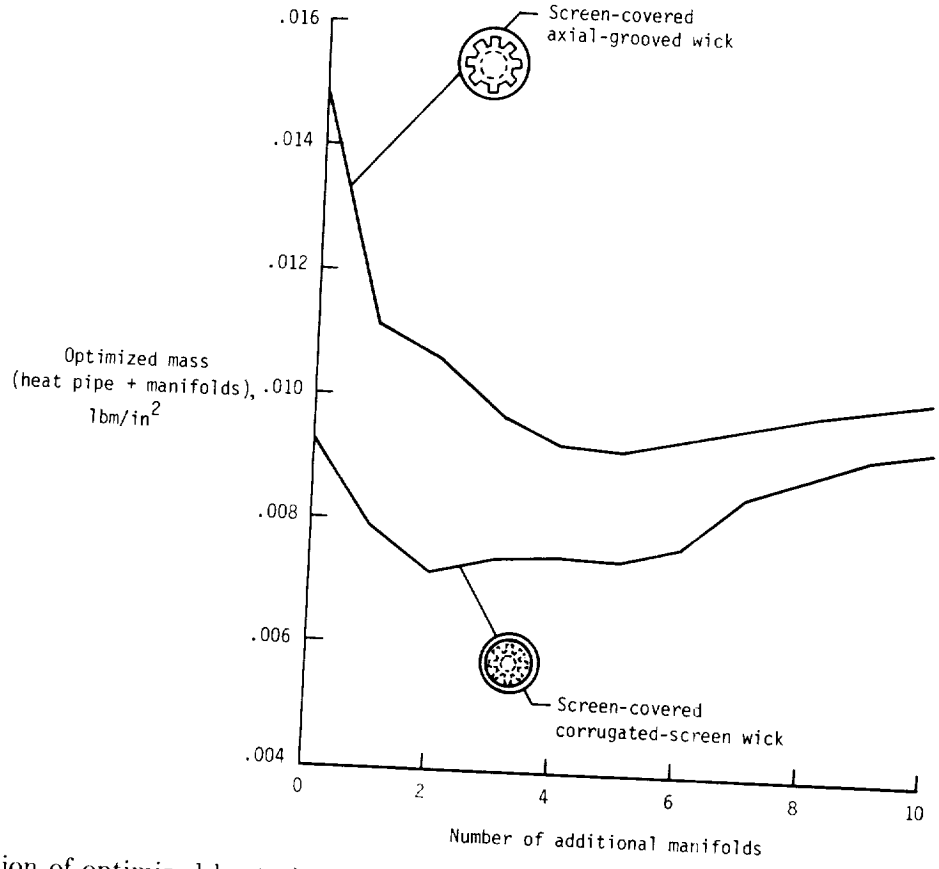

Figure 12. Variation of optimized heat-pipe mass with number of additional coolant manifolds. (Cylindrical heat pipe embedded in honeycomb sandwich panel.)

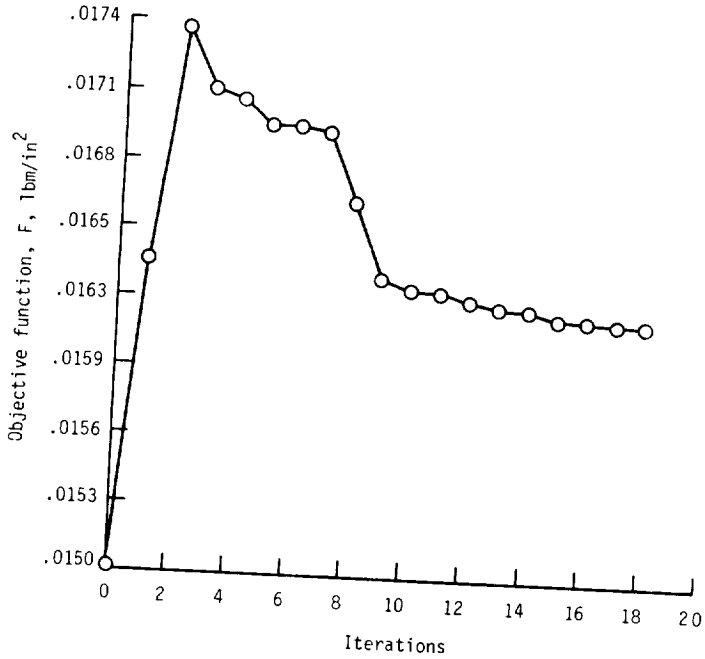

Figure 13. Objective function iteration histories (web-core sandwich with corrugated-screen composite wick with no additional coolant manifolds).

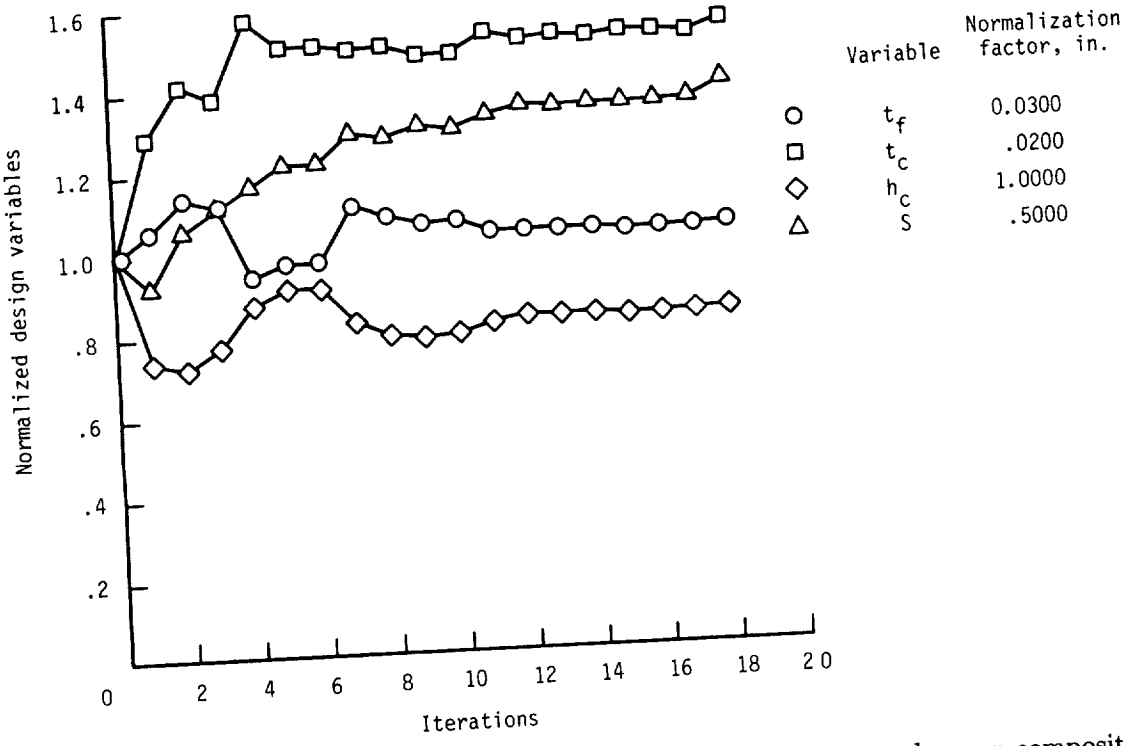

Figure 14. Design-variable iteration histories (web-core sandwich with corrugated-screen composite wick with no additional coolant manifolds).

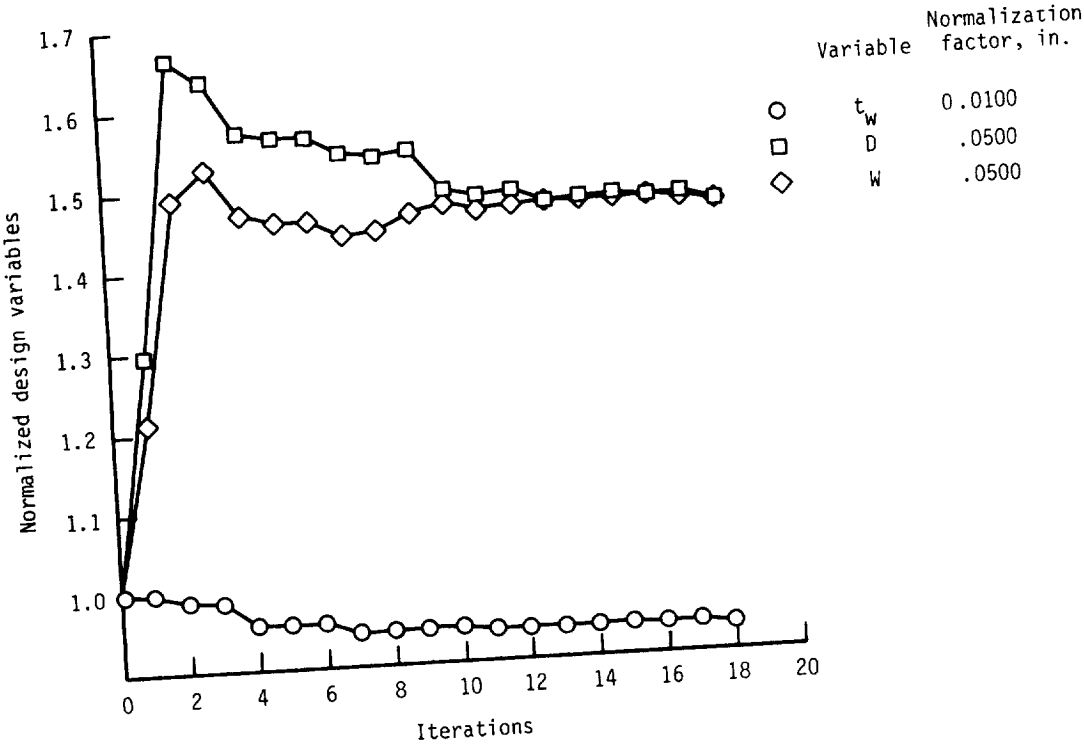

Figure 14. Concluded.

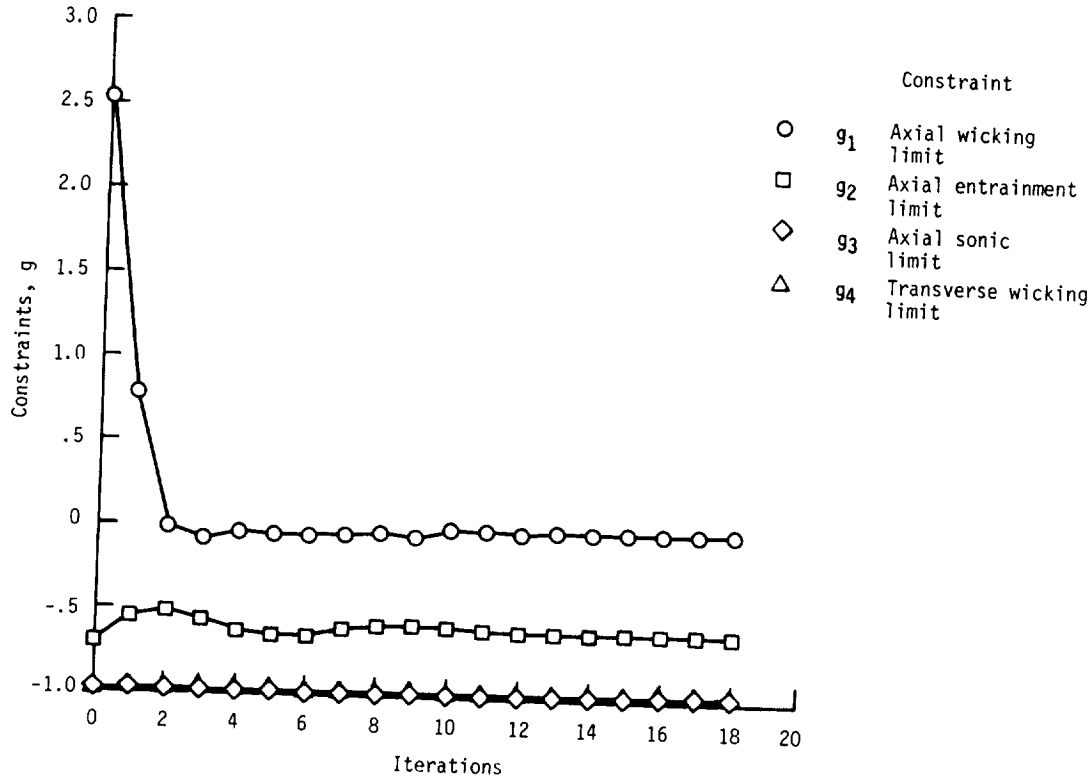

Figure 15. Constraint iteration histories (web-core sandwich with corrugated-screen composite wick and no additional coolant manifolds).

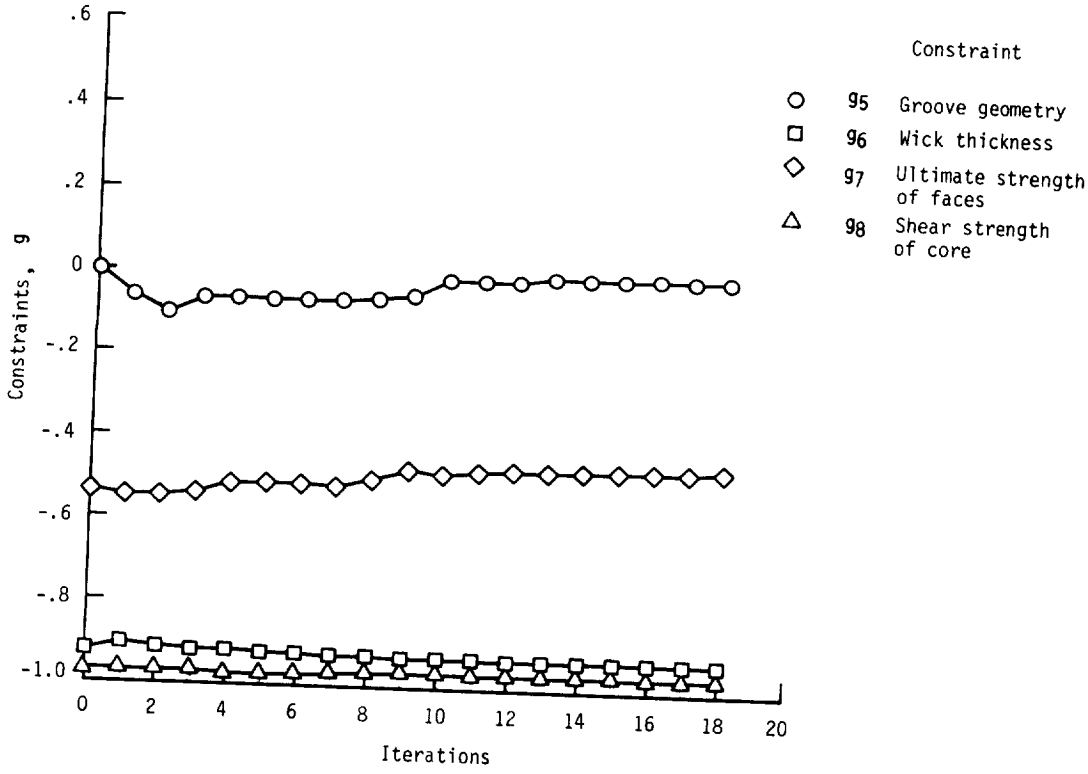

Figure 15. Continued.

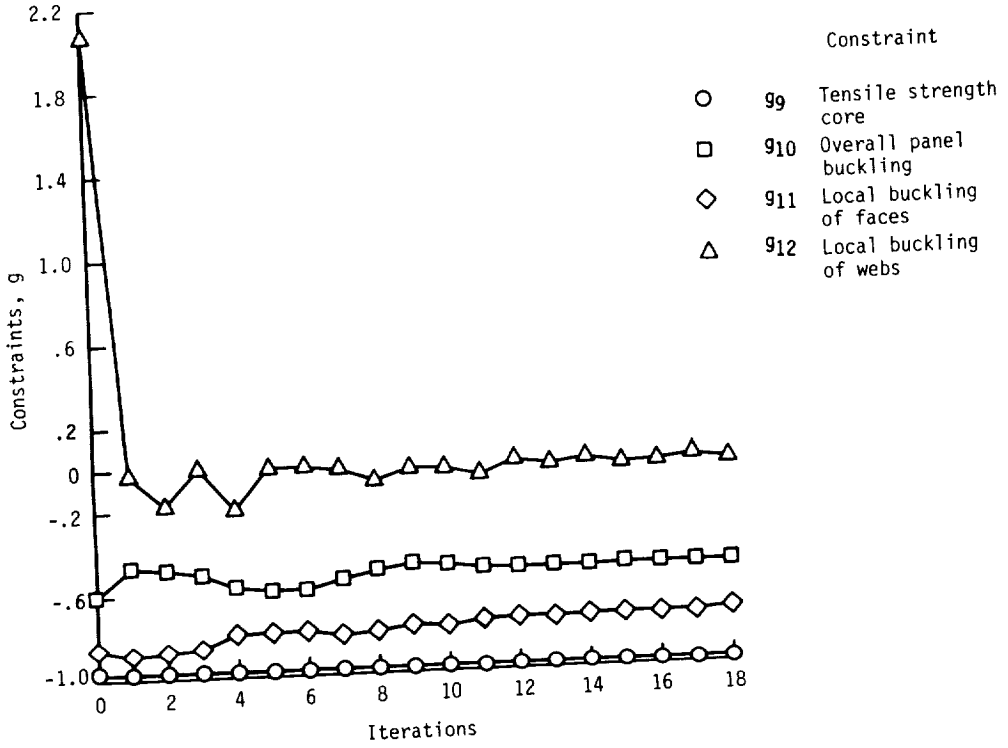

Figure 15. Continued.

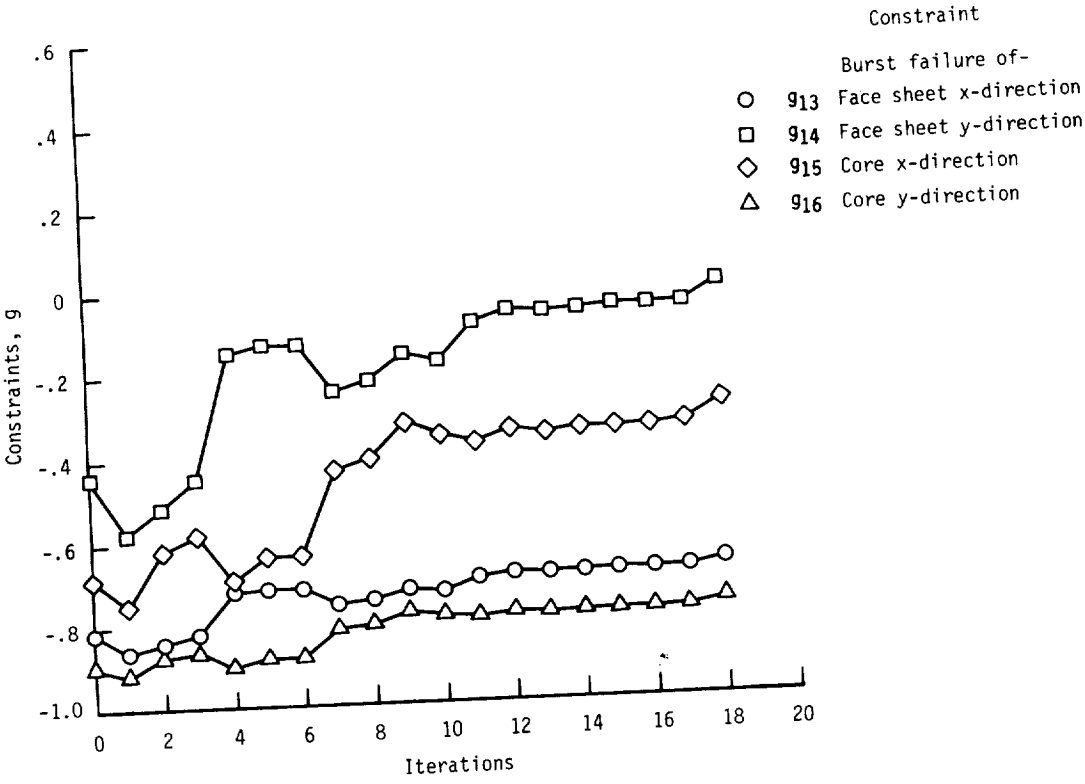

Figure 15. Continued.

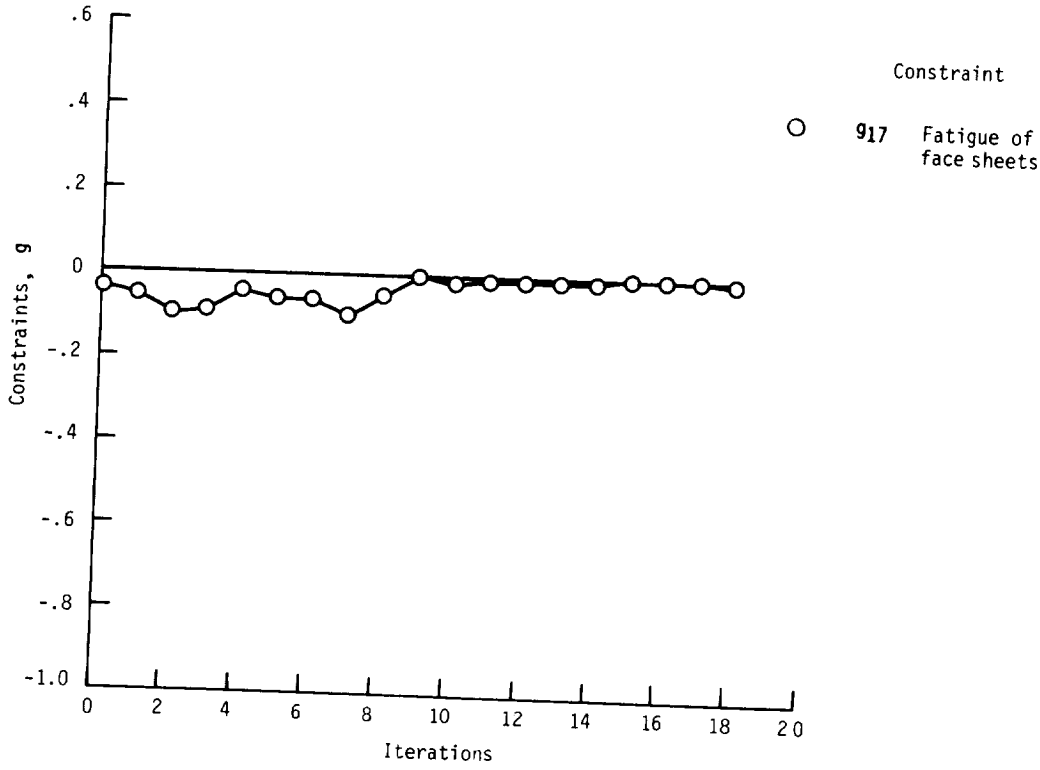

Figure 15. Concluded.

NASA
National Aeronautics and Space Administration

Report Documentation Page

1. Report No.	2. Government Accession No.	3. Recipient's Catalog No.
NASA TM-89131		

4. Title and Subtitle	5. Report Date
Application of Formal Optimization Techniques in Thermal/Structural Design of a Heat-Pipe-Cooled Panel for a Hypersonic Vehicle	October 1987
	6. Performing Organization Code
7. Author(s)	8. Performing Organization Report No.
Charles J. Camarda and Michael F. Riley	L-16134
	10. Work Unit No.
9. Performing Organization Name and Address	505-62-81-05
NASA Langley Research Center Hampton, VA 23665-5225	11. Contract or Grant No.
	13. Type of Report and Period Covered
12. Sponsoring Agency Name and Address	Technical Memorandum
National Aeronautics and Space Administration Washington, DC 20546-0001	14. Sponsoring Agency Code

15. Supplementary Notes
Charles J. Camarda: Langley Research Center, Hampton, Virginia.
Michael F. Riley: PRC Kentron, Inc., Hampton, Virginia.

16. Abstract

Nonlinear mathematical programming methods are used to design a radiantly cooled and heat-pipe-cooled panel for a Mach 6.7 transport. The cooled portion of the panel is a hybrid heat-pipe/actively cooled design which uses heat pipes to transport the absorbed heat to the ends of the panel where it is removed by active cooling. The panels are optimized for minimum mass and to satisfy a set of heat-pipe, structural, geometric, and minimum-gage constraints. Two panel concepts are investigated: cylindrical heat pipes embedded in a honeycomb core and an integrated design which uses a web-core heat-pipe sandwich concept. The latter concept was lighter and resulted in a design which was less than 10-percent heavier than an all actively cooled concept. The heat-pipe concept, however, is redundant and can sustain a single-point failure, whereas the actively cooled concept cannot. An additional study was performed to determine the optimum number of coolant manifolds per panel for a minimum-mass design.

17. Key Words (Suggested by Authors(s))	18. Distribution Statement
Heat pipes Active cooling Hypersonic vehicles Thermal/structural optimization Nonlinear mathematical programming	[redacted] Subject Category 34

19. Security Classif.(of this report)	20. Security Classif.(of this page)	21. No. of Pages	22. Price
Unclassified	Unclassified	30	